WRI-08-RO10

# EVALUATION OF BOC'S LOTOX™ PROCESS FOR THE OXIDATION OF ELEMENTAL MERCURY IN FLUE GAS FROM A COAL-FIRED BOILER

## TOPICAL REPORT

**Start Date 2005**
**End Date 2008**

**By Khalid Omar**

**May 2008**

**Jointly Sponsored Research Proposal**
**Task 65 Topical Report under DE-FC26-98FT40323**

**For**
**Linde Group**
**Murry Hill, NJ**

**And**
**U.S. Department of Energy**
**National Energy Technology Laboratory**
**Morgantown, West Virginia**

**By**
**Western Research Institute**
**Laramie, Wyoming**

**Kamalendu Das**
**Task 65**

## DISCLAIMER

## ABSTRACT

Linde's Low Temperature Oxidation (LoTOx™) process has been demonstrated successfully to remove more than 90% of the NOx emitted from coal-fired boilers. Preliminary findings have shown that the LoTOx™ process can be as effective for mercury emissions control as well. In the LoTOx™ system, ozone is injected into a reaction duct, where NO and $NO_2$ in the flue gas are selectively oxidized at relatively low temperatures and converted to higher nitrogen oxides, which are highly water soluble. Elemental mercury in the flue gas also reacts with ozone to form oxidized mercury, which unlike elemental mercury is water-soluble. Nitrogen oxides and oxidized mercury in the reaction duct and residual ozone, if any, are effectively removed in a wet scrubber. Thus, LoTOx™ appears to be a viable technology for multi-pollutant emission control.

To prove the feasibility of mercury oxidation with ozone in support of marketing LoTOx™ for multi-pollutant emission control, Linde has performed a series of bench-scale tests with simulated flue gas streams. However, in order to enable Linde to evaluate the performance of the process with a flue gas stream that is more representative of a coal-fired boiler; one of Linde's bench-scale LoTOx™ units was installed at WRI's combustion test facility (CTF), where a slipstream of flue gas from the CTF was treated. The degree of mercury and NOx oxidation taking place in the LoTOx™ unit was quantified as a function of ozone injection rates, reactor temperatures, residence time, and ranks of coals.

The overall conclusions from these tests are: 1) over 80% reduction in elemental mercury and over 90% reduction of NOx can be achieved with an $O_3/NO_X$ molar ratio of less than two, 2) in most of the cases, a lower reactor temperature is preferred over a higher temperature due to ozone dissociation, however, the combination of both low residence time and high temperature proved to be effective in the oxidation of both NOx and elemental mercury, and 3) higher residence time, lower temperature, and higher molar ratio of $O_3$/NOx contributed to the highest elemental mercury and NOx reductions.

## TABLE OF CONTENTS

## TABLES AND FIGURES

## EXECUTIVE SUMMARY

Linde's Low Temperature Oxidation (LoTOx™) process has been demonstrated successfully to remove more than 90% of the NOx emitted from coal-fired boilers. Preliminary findings have shown that the LoTOx™ process can be as effective for mercury emissions control as well. In the LoTOx™ system, ozone is injected into a reaction duct, where NO and $NO_2$ in the flue gas are selectively oxidized at relatively low temperatures and converted to higher nitrogen oxides, which are highly water soluble. Elemental mercury in the flue gas also reacts with ozone to form oxidized mercury, which unlike elemental mercury is water-soluble. Nitrogen oxides and oxidized mercury in the reaction duct and residual ozone, if any, are effectively removed in a wet scrubber. Thus, LoTOx™ appears to be a viable technology for multi-pollutant emission control.

To prove the feasibility of mercury oxidation with ozone in support of marketing LoTOx™ for multi-pollutant emission control, Linde has performed a series of bench-scale tests with simulated flue gas streams. However, in order to enable Linde to evaluate the performance of the process with a flue gas stream that is more representative of a coal-fired boiler; one of Linde's bench-scale LoTOx™ units was installed at WRI's combustion test facility (CTF), where a slipstream of flue gas from the CTF was treated. The degree of mercury and NOx oxidation taking place in the LoTOx™ unit was quantified as a function of ozone injection rates, reactor temperatures, residence time, and ranks of coals.

The overall conclusions from these tests are: 1) over 80% reduction in elemental mercury and over 90% reduction of NOx can be achieved with an $O_3/NO_X$ molar ratio of less than two, 2) in most of the cases, a lower reactor temperature is preferred over a higher temperature due to ozone dissociation, however, the combination of both low residence time and high temperature proved to be effective in the oxidation of both NOx and elemental mercury, and 3) higher residence time, lower temperature, and higher molar ratio of $O_3$/NOx contributed to the highest elemental mercury and NOx reductions.

## INTRODUCTION

Linde's LoTOx™ process has been demonstrated successfully to remove more than 90% of the NOx emitted from coal-fired boilers [1, 2]. Preliminary findings have shown that the LoTOx™ system can be as effective for mercury emissions control. In the LoTOx™ system, ozone is injected into a reaction duct where NO and $NO_2$ in the flue gas at relatively low temperatures are selectively oxidized and converted to higher nitrogen oxides, which are highly water soluble. Elemental mercury in the flue gas also reacts with ozone to form oxidized mercury, which unlike elemental mercury, is water-soluble. Nitrogen oxides and oxidized mercury in the reaction duct and residual ozone, if any, are effectively removed in a wet scrubber. Thus, LoTOx™ appears to be a viable technology for multi-pollutant emission control.

To prove the feasibility of mercury oxidation with ozone in support of marketing LoTOx™ for multi-pollutant emission control, Linde has performed a series of bench-scale tests focusing on the evaluation of the LoTOx™ system for elemental mercury oxidation and removal. In these tests, ozone was added to a simulated flue gas stream that was doped with ppb levels of elemental mercury. The stream then entered a heated quartz reactor, and the degree of mercury oxidation was determined for different reactor operating conditions.

To enable Linde to evaluate the performance of the process with a flue gas stream that is more representative of a coal-fired boiler, the Combustion Test Facility (CTF) at Western Research Institute (WRI) was utilized to generate a slipstream of flue gas for Linde's bench-scale LoTOx™ unit.

The overall goal of the project is to determine the ability of the LoTOx™ process to oxidize elemental mercury contained in coal-derived flue gas, under different operating conditions. The specific objective is to evaluate the LoTOx™ technology in its degree of oxidizing elemental mercury under different ozone injection rates, residence time, and temperatures utilizing flue gas generated from the combustion of a western sub-bituminous coal and an eastern bituminous coal.

## OBJECTIVES

The overall goal of the project is to determine the ability of the LoTOx™ process to oxidize elemental mercury contained in coal-derived flue gas, under different operating conditions.

Specific objectives are to:

1- Install bench-scale LoTOx™ unit in Combustion Test Facility,

2- Operate LoTOx™ unit under different ozone injection rates and temperatures, and characterize mercury oxidation, and

3- Test process with both a western sub-bituminous coal and an eastern bituminous coal.

## EXPERIMENTAL SET UP

### COMBUSTION TEST FACILITY

The WRI coal combustion test facility (CTF) is a nominal 250,000 Btu/hr balanced-draft system designed to replicate a pulverized coal-fired utility boiler. A schematic of the CTF is shown in Figure 1. In its present configuration, the unit is set up to simulate a tangential-fired boiler, but may be easily adapted to wall-fired or other configurations. The fuel feed system consists of screw-based feeders and pneumatic transport to four burners inserted in the corners of a refractory-lined firebox. The burners can be angled to attain different tangential flow characteristics in the firebox. The unit is equipped with appropriately sized heat-recovery surfaces such that the time/temperature profile of a utility boiler is replicated. These surfaces comprise water-cooled panels that simulate the waterwall, an air-cooled superheater, preheater, and two economizers. CTF includes provisions for preheating the combustion air to mimic a utility air preheater. The system also includes over-fire air injection ports for combustion staging. The unit is equipped with two baghouses for continuous fly ash removal and with an inertia separation probe of fly ash (QSIS$^{TM}$) for "clean" sampling under different steady-state operations. Figure 2 shows a photograph of the facility as installed at WRI facilities.

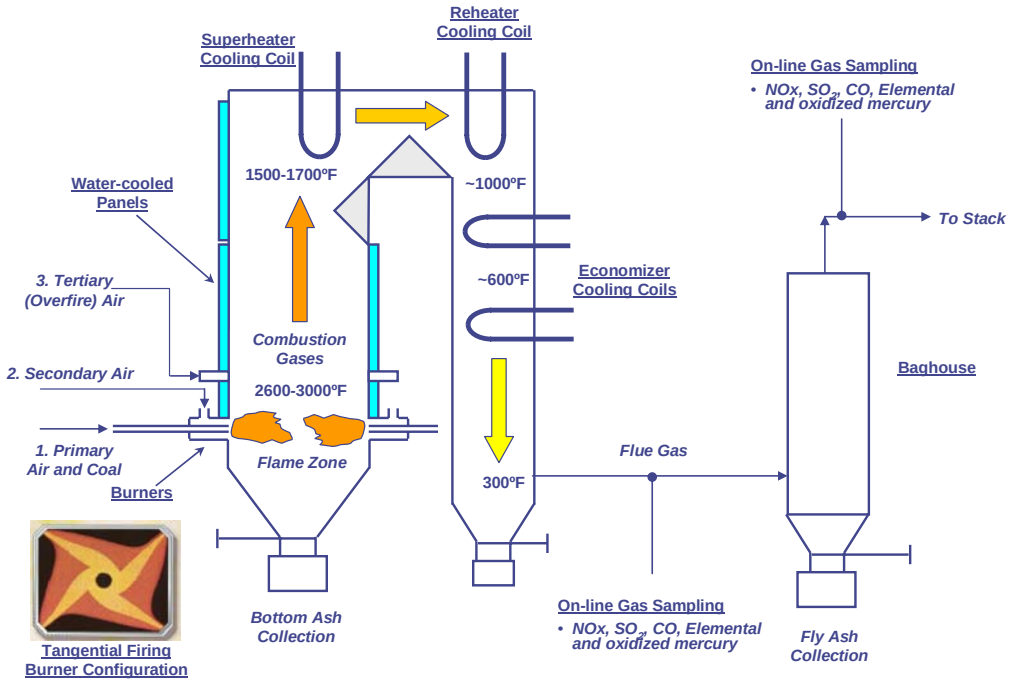


**Figure 1. A Schematic of the Combustion Test Facility**

**Figure 2. A Photograph of the CTF**

Continuous monitoring and recording (i.e., 10 second increments) of process parameters and gas concentrations (i.e., $SO_2$, NOx, CO, $O_2$) are accomplished through a PC-based data acquisition system. Carbon dioxide and nitrogen concentrations in the flue gas are determined by gas chromatograph analysis of sample bombs withdrawn at regular intervals. A Testo analyzer is also available for $CO_2$, CO, $SO_2$, NOx monitoring as and when required. Flue gas samples can be taken from several locations. Filtration of fly ash from samples withdrawn is accomplished using a temperature controlled inertial separation probe. Samples are then chilled for dew point control and then pumped to the analysis train. All analyzers are calibrated regularly with EPA protocol gas with ±1% accuracy of the reported concentration. Isokinetic fly ash samples can be taken from several locations upstream of the baghouse.

The LoTOx$^{TM}$ bench scale unit was integrated with the coal combustion test facility at WRI. The process flow diagram of the CTF presented in Figure 3 reflects the location of the slip stream of flue gas that was supplied from the CTF to the LoTOx$^{TM}$ unit. A schematic and a picture of the LoTOx$^{TM}$ experiment are shown in Figures 4 and 5.

In these set of tests, a bituminous and a subbituminous coal was utilized. A complete analysis for coal used is listed in Appendix A.

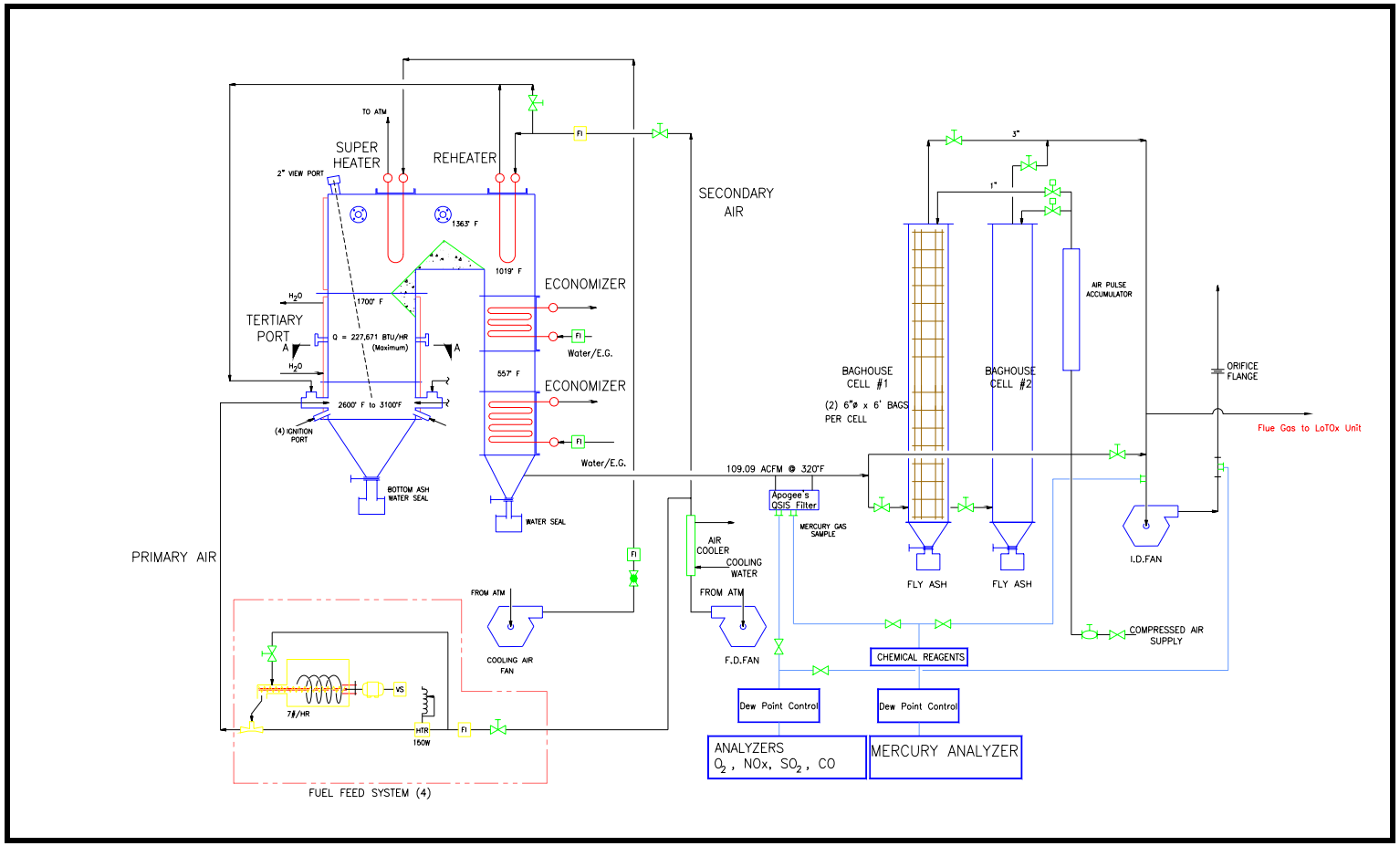


**Figure 3. Process Flow Diagram of the Combustion Test Facility**

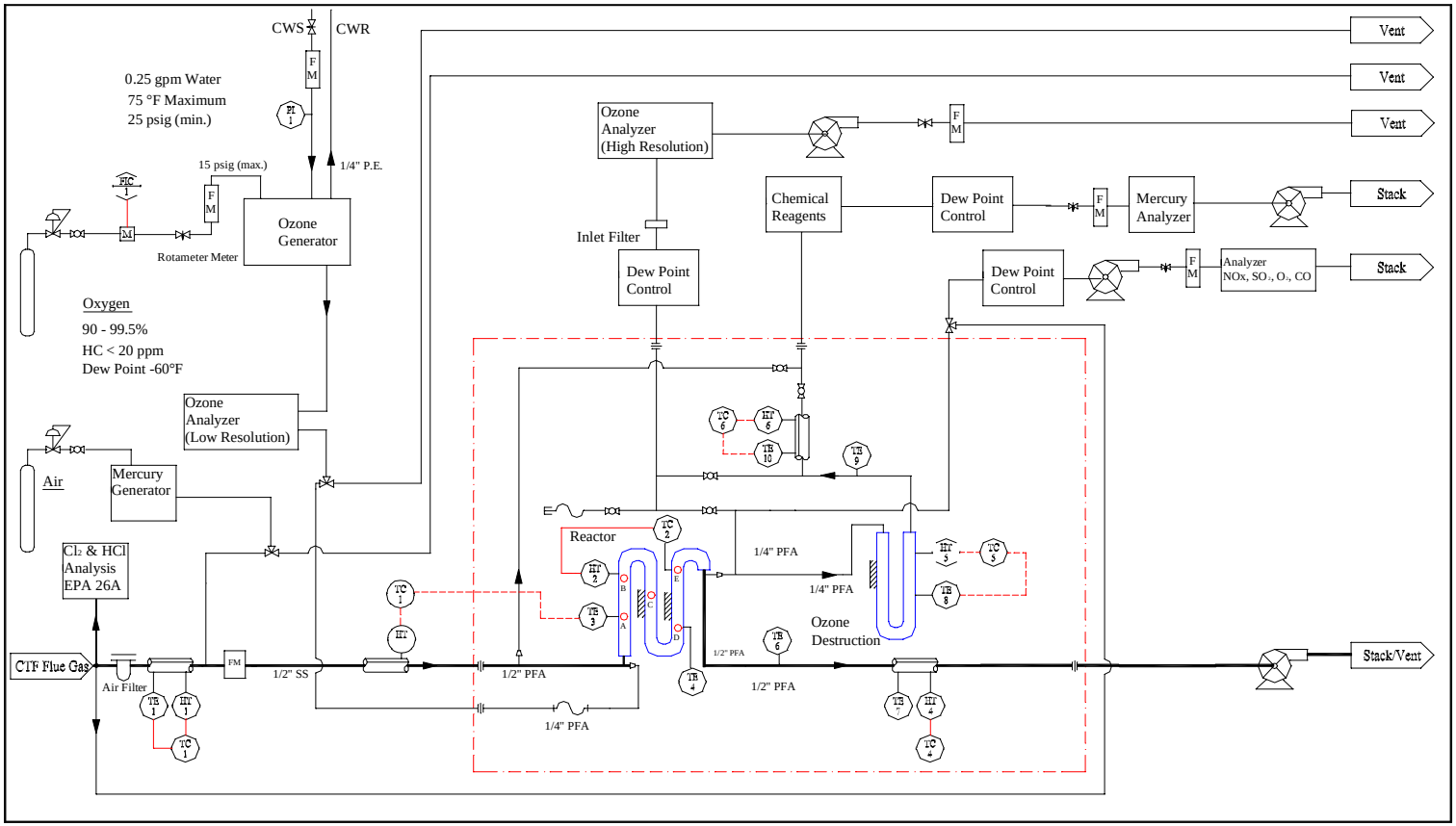


**Figure 4. Schematic of the LoTOx™ as Integrated with the Combustion Test Facility**

**Figure 5. Picture of the LoTOx™ Unit**

The bench scale LoTOx$^{TM}$ unit consists of quartz reactor, gas analysis system for NOx, $SO_2$, $O_3$, CO, $O_2$, mercury analysis train, ozone injection system, and ozone destruction reactor. A description of these components is a follows:

Quartz Reactor

Due to the negligible reactivity with mercury, a quartz reactor was utilized in these tests. A dimensional drawing of the reactor is illustrated in Figure 6. The reactor is equipped with multiple ports for ozone injection to control the residence time of the reaction. The thermally insulated reactor was maintained at fixed temperature throughout the reactor by controlling the inlet and exit temperatures using two separate temperature controllers.

Gas Analysis Train

A list of various analyzers used for measuring the flue gas constituents is given in Table 1. Each instrument is regularly and routinely calibrated. Typically, the calibration process takes place during the beginning of the test day and is then checked throughout the test process. Comparisons between the measurements of the continuous emission mercury analyzer and the carbon sorbent traps (EPA method 30B) indicate the high reliability and accuracy of the mercury analyzer utilized in these tests.

**Table 1. List of Analyzers used for Flue Gas Measurements**

| Analyzer | Basis for Analysis | Brand/Model No. |
|---|---|---|
| $SO_2$ | Photometric | Bovar Engineered Products/Model 721M |
| NOx | Chemiluminescence | Thermo Environmental Instruments/Model 42H |
| CO | NDIR | Fuji Model 3300 |
| $O_2$ | Paramagnetic | M&C Instruments/PMA 22 |
| $O_3$ (High Resolution) | Photometric | Advanced Pollution Instruments/Model 450 |
| $O_3$ (Low Resolution) | | Ozone Instrumentation AFx Model H1 |
| Halides & Halogens | EPA Method 26A | N/A |

Mercury Analysis System

The mercury analysis train utilized is in accordance with the test method developed at Linde. The analysis train consists of a continuous emission monitor mercury analyzer, sample conditioner (water dew point control) and a wet impinger train for speciation of mercury and removal of $SO_2$ due to its interference with the mercury analyzer measuring technique.

The mercury analyzer used is a model VM-3000 manufactured by Mercury Instruments. The measuring technique is based on the UV absorption of elemental mercury. The impinger train consists of a solution of potassium chloride to absorb oxidized mercury, followed by a solution of sodium bicarbonate to absorb $SO_2$. In all the tests conducted, only the concentration of elemental mercury was measured.

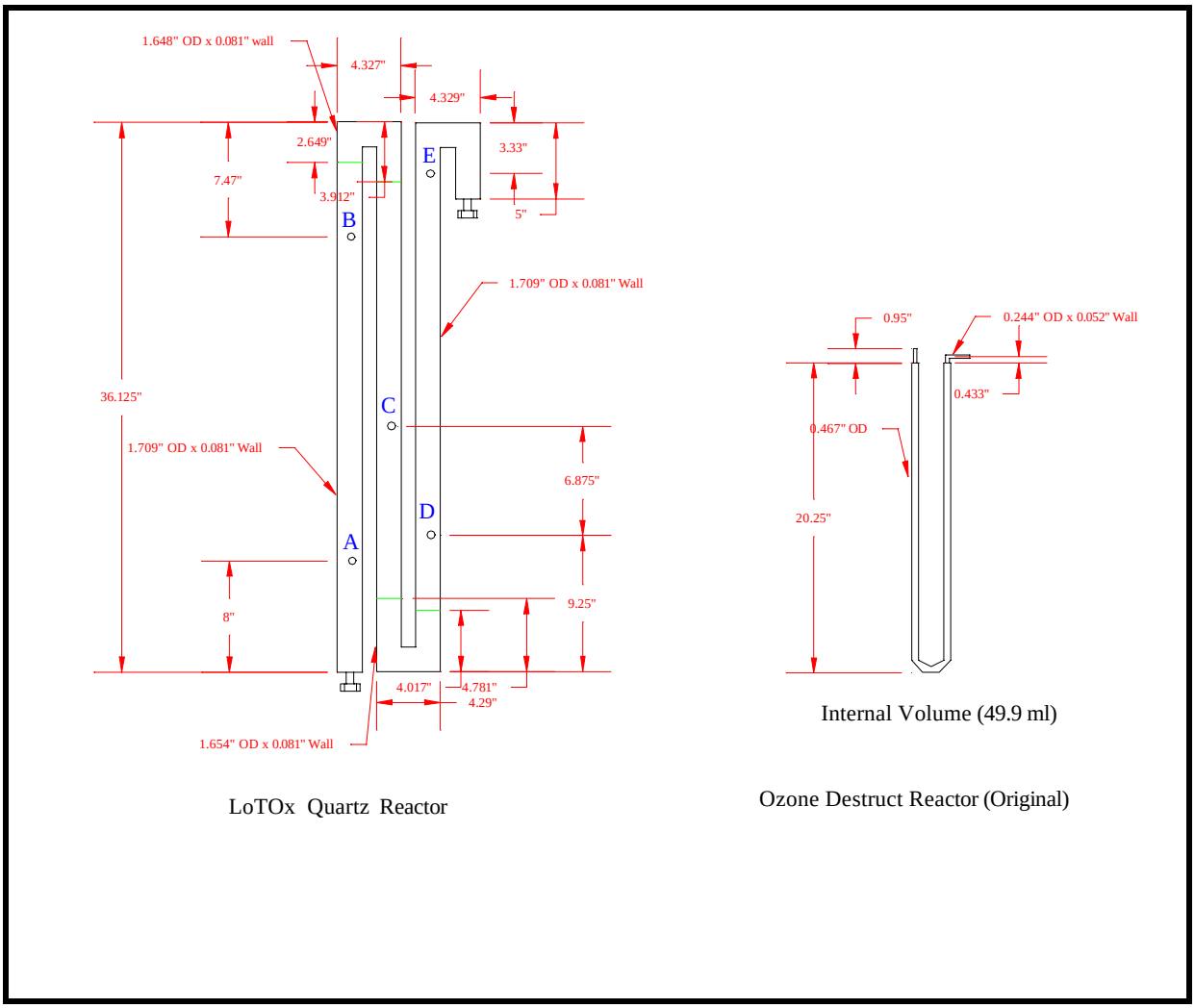


**Figure 6. Dimensions of the Reactor and the Ozone Destruction Unit**

Ozone Injection System

The ozone is generated by passing dry oxygen (i.e., dew point of water -40 $^{o}$F) through a plasma reactor. The flow rate of the outlet oxygen stream from the ozone generator is controlled using a mass flow controller and the percentage of ozone present in the oxygen stream is determined using a low resolution ozone analyzer. The excess ozone downstream of the reactor was monitored using a high resolution ozone analyzer.

Ozone Destruction Reactors

Due to the interference of ozone with elemental mercury measurements, the samples has to be heated to over 500 $^{o}$F to ensure full dissociation of ozone. Figure 6 shows the quartz ozone destruction reactor used in the tests. The internal volume of the quartz reactor is 50 $cm^3$. Due to concerns over reaction taking place in the ozone destruction reactor, two more reactors were built, the first was utilized to determine the temperature required to fully destruct the ozone, and the second was utilized to confirm the results of the tests conducted with the quartz reactor. This reactor has an internal volume 7 $cm^3$ and is constructed from stainless steel. Detail of the results of these tests is shown in Appendix D.

## EXPERIMENTAL PROCEDURE

In reference to Figure 4, the following procedure was implemented in the tests conducted:

- Calibration of the analyzers with standard gases.
- Allow flow and temperature of air at the targeted reaction temperature in the quartz reactor to reach a steady state.
- Switch from air to flue gas then allow enough time to achieve a steady state condition.
- Leak check by determining the oxygen concentration in and out of the reactor and after the ozone destruction unit. The LoTOx$^{TM}$ unit is maintained at slight vacuum and any air infiltration will be shown in the exit oxygen concentrations from the reactor and the ozone destruction unit.
- Inject mercury from the mercury generator to reach an inlet concentration of 12 $\mu g/m^3$ of mercury in the flue gas and allow the outlet concentration of mercury from the reactor to reach a steady state.
- The mass flow rate of flue gas is determined by injecting a know amount of oxygen using an oxygen mass flow meter and then determining the oxygen concentration before and after the injection location using the oxygen analyzer. This process was part of the sequence for each test that was conducted.
- Inject ozone through one of the injection ports in the reactor that corresponds to the targeted residence time.
- Adjust the power of the ozone generator to reach the required $O_3$/NOx molar ratio.

Test Sequence:

The test sequence involves the measuring of the concentration of flue gas and elemental mercury from the inlet and the outlet sides of the reactor according to the following sequence: Baseline (Inlet to Reactor) ⇒ Baseline (Outlet from the Reactor) ⇒Test (Inject Ozone) ⇒Baseline (Outlet from the Reactor) ⇒ Baseline (Inlet to Reactor)

A minimum of 20 minutes of steady state condition of elemental mercury concentration level was allowed for each test. Figure 7 is a graphical illustration of the test sequence.

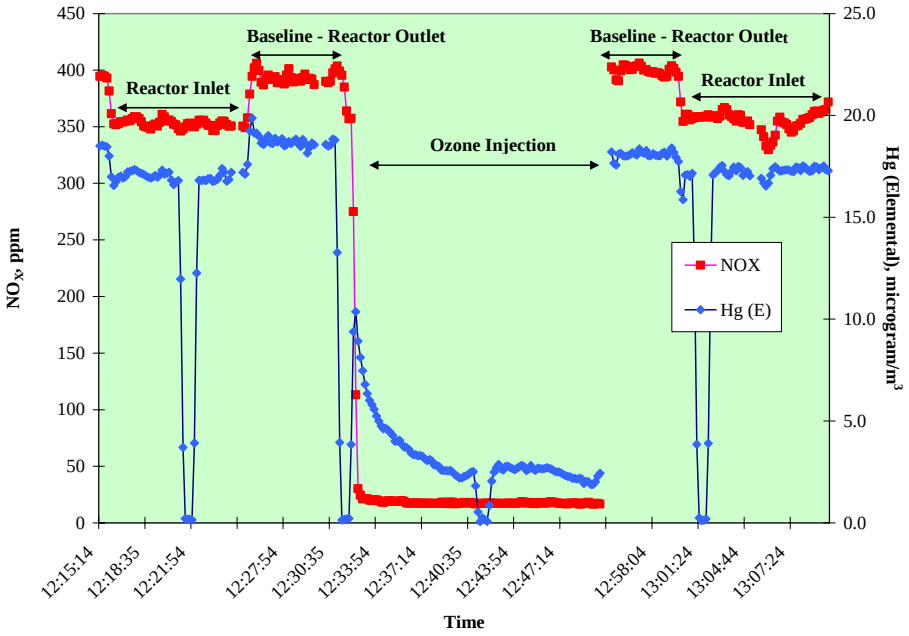


**Figure 7. Graphical Illustration of the Trends during Test**

Data Logged/Recorded during the Test

- Elemental mercury and $NO_X$ concentrations before and after the reactor.
- Ozone concentration in the flue gas downstream of the reactor.
- Ozone concentration in the inlet oxygen stream.
- Temperatures at several ports in the reactor.
- The mass flow rate of oxygen.
- Ozone injection port.

## RESULTS & DISCUSSION

A parametric study was conducted to delineate the effect of residence time, $O_3$/NOx stoichiometric ratio, temperature, and coal rank on the oxidation of both elemental mercury and NOx.

The ranges for the three major variables investigated are listed in Table 2. Following is a brief discussion of the data.

**Table 2. Process Variables**

| Process Variable | Range |
|---|---|
| Reaction Temperature | 150 $^{o}$F & 275 $^{o}$ F |
| $O_3$/NOx Molar Ratio | 1.0 to 4.0 |
| Residence time | 0.5 seconds (low residence time, LRT to 〉 5 seconds (high residence time, HRT) |

NOx Conversion

Conversion of NOx to higher oxides was quantified as a function of residence time, temperature, molar ratio of $O_3$/NOx, and the rank of coal. The results of these tests are presented in Tables 3-5 and graphically illustrated in Figure 8. Figure 8 shows the amount of NOx conversion as percent NOx reduction vs. $O_3$/NOx stoichiometric ratio. The conclusions from the data displayed in the Tables and in the Figure are:

- There is no clear effect of the rank of coal in the degree of NOx oxidation.
- The increase in temperature from 150 $^{o}$F to 275 $^{o}$F had a small effect in the degree of NOx oxidation.
- As expected, the increase in both the residence time and $O_3$/NOx stoichiometric ratio increased the degree of NOx oxidation.
- About 90% oxidation level of NOx at 150 $^{o}$F was achieved with bituminous coal at $O_3$/NOx stoichiometric molar ratio of two. For subbituminous coal, over 95% NOx reduction was achieved at similar operating conditions (refer to Appendix D, Table 13).

Elemental Mercury Reduction

The effect of the coal rank, $O_3$/NOx molar ratio, temperature, residence time on elemental mercury reduction was evaluated based on the experimental results in Tables 3-5. Note that the inlet mercury concentration was maintained at nearly 12 $\mu g/m^3$ during all the tests, however, the reported value is higher since it is adjusted for comparison reasons to 3% oxygen. The percentage conversion of Hg (E) is highly dependent on the inlet Hg (E) concentration, and tends to be lower at lower inlet concentrations. The effect of each major process variable is considered below.

Coal Rank

The two ranks of coals tested have different chlorine and sulfur levels. The average concentration of $SO_2$ in the flue gas generated from bituminous coal combustion is 560 ppm (adjusted to 3% $O_2$), while for subbituminous coal, it ranged from 230 ppm to 350 ppm.

## Table 3. Results of the LoTOx™ Tests with Bituminous Coal

| | Reactor Temp. °F | Ozone Injection Port | Residence Time Seconds | $O_3$/NOx | Excess $O_3$ out ppm | NOx (out) Prior ppm | NOx (out) Post ppm | NOx (average) Baseline ppm | Hg (E) (out) Prior μg/m³ | Hg (E) (out) Post μg/m³ | Hg (E) (average) Baseline μg/m³ | NOx Test ppm | Hg (E) Test μg/m³ | NOx Reduction % | Hg (E) Reduction % |
|---|---|---|---|---|---|---|---|---|---|---|---|---|---|---|---|
| Test 1 | 150 | A | 5.62 | 1.42 | 68 | 354 | 381 | 368 | 18.9 | 18.0 | 18.5 | 60 | 6.8 | 83.7 | 63.0 |
| Test 2 | 150 | A | 5.99 | 2.44 | 317 | 389 | 399 | 394 | 18.6 | 18.1 | 18.3 | 18 | 2.8 | 95.4 | 84.7 |
| Test 3 | 150 | E | 0.54 | 1.46 | 62 | 422 | 449 | 436 | 18.7 | 19.2 | 19.0 | 215 | 8.9 | 50.6 | 53.0 |
| Test 4 | 150 | E | 0.52 | 2.50 | 288 | 370 | 430 | 400 | 19.6 | 19.9 | 19.8 | 83 | 6.8 | 79.3 | 65.4 |
| Test 5 | 275 | E | 0.43 | 1.45 | 43 | 378 | 404 | 391 | 16.0 | 17.1 | 16.6 | 183 | 7.4 | 53.2 | 55.6 |
| Test 6 | 275 | E | 0.44 | 2.39 | 285 | 399 | 371 | 385 | 17.6 | 17.9 | 17.8 | 69 | 5 | 82.1 | 72.1 |
| Test 7 | 275 | A | 5.52 | 2.10 | 50 | 371 | 348 | 360 | 18.2 | 17.8 | 18.0 | 53 | 2.6 | 85.3 | 85.4 |
| Test 8 | 275 | A | 5.96 | 4.35 | 288 | 336 | 350 | 343 | 17.0 | 16.9 | 17.0 | 7 | 1.4 | 98.0 | 92.0 |

## Table 4. Results of the LoTOx™ Tests with Subbituminous Coal at Low Temperature

| | Reactor Temp. °F | Ozone Injection Port | Residence Time second | $O_3$/NOx | Excess $O_3$ out ppm | NOx (out) Prior ppm | NOx (out) Post ppm | NOx (average) Baseline ppm | Hg (E) (out) Prior μg/m³ | Hg (E) (out) Post μg/m³ | Hg (E) (average) Baseline μg/m³ | NOx Test ppm | Hg (E) Test μg/m³ | NOx Reduction % | Hg (E) Reduction % |
|---|---|---|---|---|---|---|---|---|---|---|---|---|---|---|---|
| Test 1 | 150 | A | 5.25 | 1.64 | 296 | - | - | - | 16.5 | 16.7 | 16.6 | - | 4.0 | - | 75.9 |
| Test 2 | 150 | A | 6.57 | 1.19 | 79 | - | - | - | 16.5 | 16.7 | 16.6 | - | 8.4 | - | 49.4 |
| Test 3 | 150 | E | 0.62 | 2.16 | 259 | - | - | - | 17.3 | 18.1 | 17.7 | - | 11.9 | - | 33.0 |
| Test 4 | 150 | E | 0.58 | 1.26 | 76 | - | - | - | 17.2 | 19.4 | 18.3 | - | 13.9 | - | 24.0 |

## Table 5. Results of the LoTOx™ Tests with Subbituminous Coal at High Temperature

| | Reactor Temp. °F | Ozone Injection Port | Residence Time second | $O_3$/NOx | Excess $O_3$ out ppm | NOx (out) Prior ppm | NOx (out) Post ppm | NOx (average) Baseline ppm | Hg (E) (out) Prior μg/m³ | Hg (E) (out) Post μg/m³ | Hg (E) (average) Baseline μg/m³ | NOx Test ppm | Hg (E) Test μg/m³ | NOx Reduction % | Hg (E) Reduction % |
|---|---|---|---|---|---|---|---|---|---|---|---|---|---|---|---|
| Test 1 | 275 | A | 6.20 | 2.70 | 71 | 268 | 353 | 311 | 16.4 | 15.5 | 16.0 | 28 | 4.0 | 90.9 | 74.9 |
| Test 2 | 275 | A | 5.73 | 3.30 | 264 | 289 | 281 | 285 | 15.7 | 15.9 | 15.8 | 3 | 2.3 | 98.9 | 85.7 |
| Test 3 | 275 | E | 0.45 | 1.36 | 67 | 292 | 314 | 303 | 15.8 | 16.7 | 16.2 | 139 | 9.1 | 54.2 | 43.6 |
| Test 4 | 275 | E | 0.47 | 2.31 | 294 | 315 | 367 | 341 | 17.3 | 17.1 | 17.2 | 46 | 6.9 | 86.6 | 59.5 |

**Note: Hg (E) and NOx concentrations are adjusted to 3% Oxygen**

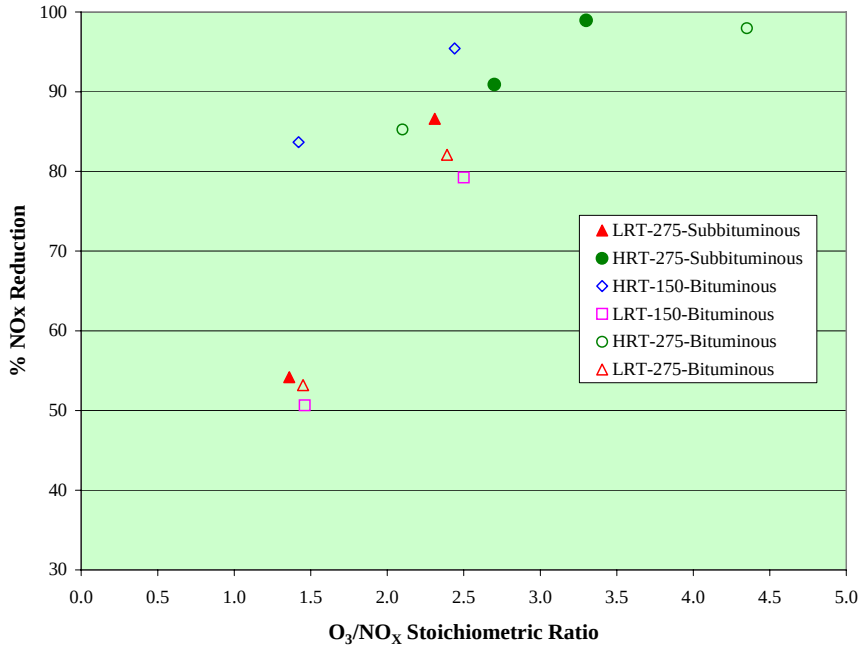


**Figure 8. NOx Reduction Data**

During these tests, a noticeable increase in $SO_2$ concentration was observed downstream of the reactor with the injection of ozone. This is attributed to interference, since both $SO_2$ and $O_3$ have similar UV absorption wave lengths. Therefore, in future tests the ozone has to be destructed before the $SO_2$ concentration is analyzed when using photometric method that is based on UV absorption.

The halide and halogen concentrations in the flue gas of both bituminous and sub bituminous coals were determined using EPA method 26A. The concentrations of halogens and halides in the flue gas for both ranks of coals are listed in Appendix C.

In order to compare the effect of the ranks of coal on elemental mercury reduction, the results of all the tests are illustrated in Figure 9 for comparison. As indicated, higher conversion of elemental mercury is observed with bituminous coal at low residence time, however at higher residence time this large variation is not significant. The high concentration of HCl in bituminous coal is expected to be responsible for the higher reduction of elemental mercury concentrations in the flue gas than with subbituminous coal.

Temperature Effect

In general, the highest mercury oxidation level was observed at low temperature and high residence time with both ranks of coals. At low residence time, the increase in temperature enhanced mercury oxidation to a high degree with subbituminous coal while is it is marginal with bituminous coal. At high residence time, the increase in reactor temperature did not produce favorable results in comparison to lower temperature. This may be attributed to sufficient residence time at high temperature for dissociation of a portion of the injected ozone.

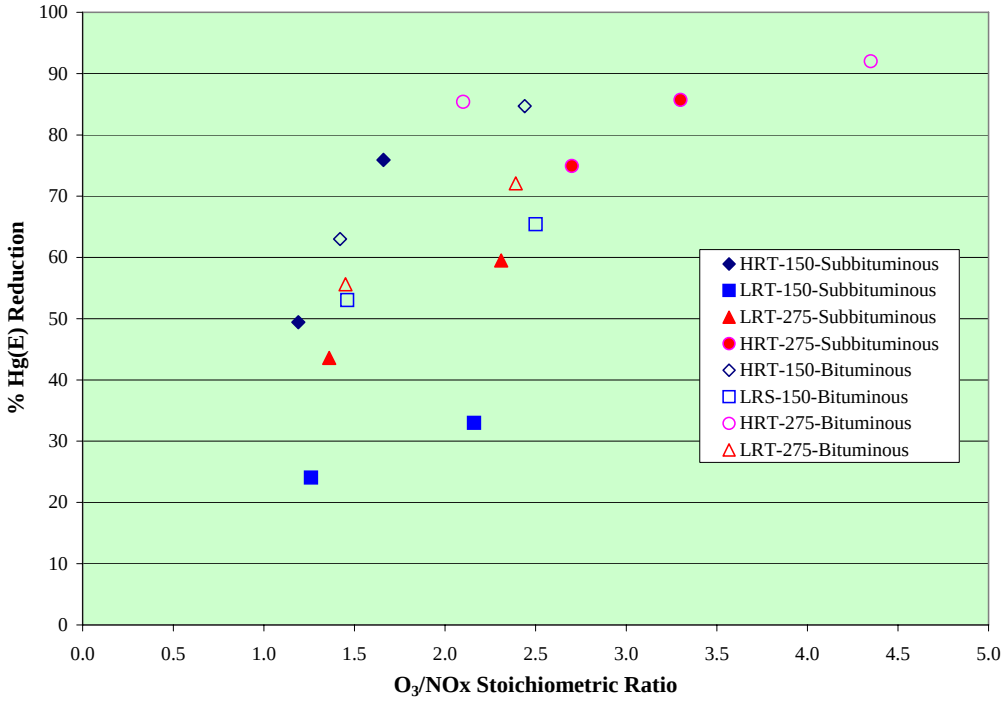


**Figure 9. Elemental Mercury Conversion Data**

Residence Time effect

In all the tests conducted, higher Hg (E) reductions were observed with higher residence time, holding the temperature and the $O_3$/NOx ratio constant.

## CONCLUSIONS

A parametric study was conducted to evaluate LoTOx$^{TM}$ process for its multipollutant reduction capabilities with particular emphasis on mercury. The parameters under consideration were the ozone injection rates, the residence time, the temperatures and the rank of coal. To evaluate this technology with a representative flue gas of conditions in power plants, a slip stream from the combustion test facility was treated in a bench-scale unit. The overall

conclusions from these tests are: 1) over 80% reduction in elemental mercury and over 90% reduction of NOx can be achieved with $O_3/NO_X$ molar ratio of about two, 2) in most of the cases, lower reactor temperature is preferred over higher temperature due to ozone dissociation, however, the combination of both low residence time and high temperature proved to be effective in the oxidation of both NOx and elemental mercury, and 3) higher residence time, lower temperature, and higher molar ratio of $O_3$/NOx contributed to the highest elemental mercury and NOx conversions.

## REFERENCES


1. Jarvis, J. B.; Day, A. T.; Suchak, N. J., "LoTOx™ Process Flexibility and Multi-Pollutant Control Capability", A&WMA, Proceeding of the Mega Symposium, May 19-22, 2003.

2. Ferrell, R. J., "A Review of Oxidation Technologies Instrumental in Simultaneous Removal of Pollutants from Flue Gas Streams", The Clearwater Coal Conference, 989-1000, 2004.

# APPENDIX A

## Coal Analysis

**Table 6. Analysis of Eastern Bituminous Coal**

| **Proximate Analysis:** | As Received | Moisture Free | MAF Basis |
|---|---|---|---|
| Moisture, wt% | 1.50 | ****** | ****** |
| Ash, wt% | 10.33 | 10.49 | ****** |
| Volatile Matter, wt% | 34.60 | 35.13 | 39.25 |
| Fixed Carbon, wt% | 53.57 | 54.38 | 60.75 |
| Total | 100.00 | 100.00 | 100.00 |

| **Ultimate Analysis:** | | | |
|---|---|---|---|
| Moisture, wt% | 1.50 | ****** | ****** |
| Hydrogen, wt% | 4.65 | 4.72 | 5.27 |
| Carbon, wt% | 76.22 | 77.38 | 86.45 |
| Nitrogen, wt% | 1.19 | 1.21 | 1.35 |
| Sulfur, wt% | 0.97 | 0.98 | 1.09 |
| Oxygen, wt% | 5.14 | 5.22 | 5.83 |
| Ash, wt% | 10.33 | 10.49 | ****** |
| Total | 100.00 | 100.00 | 100.00 |

| **Heating Value, Btu/lb** | 12,985 | 13,183 | 14,728 |
|---|---|---|---|

| **Chloride, mg/kg** | 1449 |
|---|---|

**Table 7. Analysis of Subbituminous Coal (Wyodak)**

| **Proximate Analysis:** | As Received | Moisture Free | MAF Basis |
|---|---|---|---|
| Moisture, wt% | 18.96 | ****** | ****** |
| Ash, wt% | 5.17 | 6.38 | ****** |
| Volatile Matter, wt% | 36.48 | 45.01 | 48.08 |
| Fixed Carbon, wt% | 39.39 | 48.61 | 51.92 |
| Total | 100.00 | 100.00 | 100.00 |

| **Ultimate Analysis:** | | | |
|---|---|---|---|
| Moisture, wt% | 18.96 | ****** | ****** |
| Hydrogen, wt% | 3.29 | 4.06 | 4.34 |
| Carbon, wt% | 58.44 | 72.11 | 77.02 |
| Nitrogen, wt% | 0.85 | 1.05 | 1.12 |
| Sulfur, wt% | 0.33 | 0.41 | 0.44 |
| Oxygen, wt% | 12.96 | 15.99 | 17.08 |
| Ash, wt% | 5.17 | 6.38 | ****** |
| Total | 100.00 | 100.00 | 100.00 |

| **Heating Value, Btu/lb** | 9,448 | 11,658 | 12,452 |
|---|---|---|---|

| **Chloride, mg/kg** | 9 |
|---|---|

# APPENDIX B

## Tabulated and Graphical Representation of Experimental Results

**Table 8. Detailed Results of the LoTOx™ Tests with Bituminous Coal** **Test Data :3.7.07**

| | Reactor Temp. °F | $O_2$ % | $SO_2$ ppm | NOx ppm | Hg (E) µg/m³ | $SO_2$ @3% $O_2$ ppm | CO @3% $O_2$ ppm | NOx @3% $O_2$ ppm | NOx Baseline ppm | Hg (E) @3% $O_2$ µg/m³ | Hg (E) Baseline µg/m³ | Ozone Flue Gas ppm | Excess Ozone ppm | Residence Time second | NOx % Red. | Hg (E) % Red. |
|---|---|---|---|---|---|---|---|---|---|---|---|---|---|---|---|---|
| Pre-Test 1 Baseline- RX Inlet | | 8.1 | 419 | 237 | 12.9 | 586 | 113 | 331 | | 18.2 | | | | | | |
| Pre-Test 1 Baseline- RX Outlet | | 9.0 | 418 | 237 | 12.6 | 625 | 115 | 354 | | 18.9 | | | | | | |
| Test 1 | 150 | 9.1 | 496 | 39 | 4.5 | 751 | 111 | 60 | 368 | 6.8 | 18.5 | 332 | 68 | 5.62 | 83.8 | 63.0 |
| Post Test 1- RX Outlet | | 9.0 | 423 | 254 | 12.0 | 636 | 106 | 381 | | 18.0 | | | | | | |
| Post Test 1- RX Inlet | | 7.9 | 421 | 260 | 12.5 | 578 | 97 | 356 | | 17.1 | | | | | | |
| Pre-Test 2-RX Outlet | | 9.2 | 413 | 255 | 12.2 | 630 | 104 | 389 | | 18.6 | | | | | | |
| Test 2 | 150 | 9.2 | 1055 | 11 | 1.8 | 1614 | 103 | 18 | 394 | 2.8 | 18.3 | 624 | 317 | 5.99 | 95.5 | 84.7 |
| Post Test 2- RX outlet | | 9.2 | 419 | 262 | 11.9 | 638 | 96 | 399 | | 18.1 | | | | | | |
| Post Test 2- RX inlet | | 7.7 | 425 | 260 | 12.7 | 576 | 85 | 352 | | 17.3 | | | | | | |
| Pre- Test 3- RX Outlet | | 9.3 | 406 | 273 | 12.1 | 628 | 95 | 422 | | 18.7 | | | | | | |
| Test 3 | 150 | 9.6 | 423 | 136 | 5.7 | 667 | 89 | 215 | 435 | 8.9 | 19.0 | 372 | 62 | 0.54 | 50.6 | 53.0 |
| Post Test 3- RX outlet | | 9.7 | 391 | 283 | 12.1 | 621 | 81 | 449 | | 19.2 | | | | | | |
| Post Test 3- RX Inlet | | 8.2 | 399 | 277 | 13.0 | 562 | 68 | 426 | | 18.3 | | | | | | |
| Pre-Test 4- RX Outlet | | 9.3 | 393 | 240 | 12.7 | 607 | 72 | 370 | | 19.6 | | | | | | |
| Test 4 | 150 | 9.6 | 878 | 52 | 4.3 | 1384 | 75 | 83 | 400 | 6.8 | 19.7 | 640 | 288 | 0.52 | 79.4 | 65.4 |
| Post Test 4- RX Outlet | | 9.6 | 396 | 272 | 12.6 | 626 | 67 | 430 | | 19.9 | | | | | | |
| Post Test 4/Pre Test 5- RX Inlet | | 8.2 | 403 | 264 | 9.6 | 568 | 54 | 372 | | 13.5 | | | | | | |
| Pre Test 5 - RX Outlet | | 7.3 | 469 | 288 | 12.2 | 614 | 54 | 378 | | 16.0 | | | | | | |
| Test 5 | 275 | 7.2 | 488 | 140 | 5.6 | 637 | 56 | 183 | 391 | 7.4 | 16.6 | 377 | 43 | 0.43 | 53.3 | 55.6 |
| Post Test 5- RX Outlet | | 7.2 | 476 | 310 | 13.1 | 620 | 56 | 404 | | 17.1 | | | | | | |
| Post Test 5 - RX Inlet | | 5.8 | 461 | 288 | 12.4 | 545 | 51 | 317 | | 14.7 | | | | | | |
| Pre Test 6- RX Outlet | | 7.9 | 457 | 297 | 13.2 | 626 | 60 | 399 | | 17.6 | | | | | | |
| Test 6 | 275 | 8.1 | 836 | 49 | 3.6 | 1167 | 60 | 69 | 497 | 5.0 | 17.8 | 676 | 285 | 0.44 | 86.2 | 72.1 |
| Post Test 6 Baseline- RX Outlet | | 8.2 | 432 | 423 | 12.7 | 609 | 59 | 595 | | 17.9 | | | | | | |
| Post Test 6 Baseline- RX Inlet | | 6.7 | 437 | 359 | 12.6 | 550 | 54 | 458 | | 15.8 | | | | | | |
| Pre Test 7 - RX Outlet | | 8.2 | 435 | 264 | 12.9 | 610 | 61 | 371 | | 18.2 | | | | | | |
| Test 7 | 275 | 8.1 | 473 | 38 | 1.8 | 663 | 60 | 53 | 359 | 2.6 | 18.0 | 535 | 50 | 5.52 | 85.2 | 85.4 |
| Post Baseline - RX Outlet | | 8.1 | 432 | 249 | 12.8 | 604 | 59 | 348 | | 17.8 | | | | | | |
| Post Baseline - RX inlet | | 6.1 | 453 | 249 | 12.6 | 547 | 55 | 301 | | 15.2 | | | | | | |
| Post Baseline - RX Outlet | | 7.7 | 445 | 249 | 12.6 | 593 | 59 | 336 | | 17.0 | | | | | | |
| Test 8 | 275 | 7.9 | 729 | 5 | 0.9 | 1002 | 60 | 7 | 343 | 1.4 | 17.0 | 1064 | 288 | 5.96 | 98.0 | 92.0 |
| Post Test 8- RX Outlet | | 7.9 | 440 | 255 | 12.3 | 603 | 56 | 350 | | 16.9 | | | | | | |
| Post Test 8- RX Inlet | | 6.0 | 453 | 247 | 12.9 | 545 | 53 | 298 | | 15.5 | | | | | | |

**Table 9. Detailed Results of the LoTOx™ Tests with Sub bituminous Coal at Low Temperature** **Test Date: 3.14.07**

| | Reactor Temp. °F | $O_2$ % | $SO_2$ ppm | NOx ppm | Hg (E) µg/m³ | $SO_2$ @3% $O_2$ ppm | CO @3% $O_2$ ppm | NOx @3% $O_2$ ppm | Hg (E) @3% $O_2$ µg/m³ | Hg (E) Baseline µg/m³ | Ozone Flue Gas ppm | Excess Ozone ppm | Residence Time second | Hg (E) % Red. |
|---|---|---|---|---|---|---|---|---|---|---|---|---|---|---|
| Post Baseline RX Inlet | | 6.8 | 237 | 249 | 12.8 | 300 | 19 | 316 | 16.3 | | | | | |
| Pre Baseline RX Outlet | | 7.9 | 255 | 228 | 12.0 | 351 | 7 | 315 | 16.5 | | | | | |
| Test 1 | 150 | 8.5 | 768 | 0 | 2.6 | 1106 | 131 | 0 | 4.0 | 16.6 | 402 | 296 | 5.25 | 75.9 |
| Post Baseline RX Outlet | | 8.3 | 235 | 247 | 11.8 | 333 | 12 | 353 | 16.7 | | | | | |
| Pre Baseline RX Inlet | | 6.9 | 233 | 251 | 11.9 | 297 | 11 | 320 | 15.2 | | | | | |
| Pre Baseline RX Outlet | | 8.3 | 232 | 254 | 11.7 | 329 | 12 | 360 | 16.5 | | | | | |
| Test 2 | 150 | 8.0 | 329 | 14 | 6.1 | 453 | 13 | 20 | 8.4 | 16.6 | 293 | 79 | 6.57 | 49.2 |
| Post Baseline RX Outlet | | 7.7 | 245 | 248 | 12.4 | 331 | 13 | 335 | 16.7 | | | | | |
| Post Baseline RX Inlet | | 6.0 | 248 | 254 | 12.4 | 298 | 12 | 305 | 14.9 | | | | | |
| Pre Baseline RX Outlet | | 8.7 | 233 | 276 | 11.8 | 341 | 19 | 406 | 17.3 | | | | | |
| Test 3 | 150 | 9.2 | 700 | 8 | 7.7 | 1069 | 19 | 13 | 11.9 | 17.7 | 536 | 259 | 0.62 | 33.1 |
| Post Baseline RX Outlet | | 8.9 | 225 | 299 | 12.1 | 334 | 19 | 445 | 18.1 | | | | | |
| Post Baseline RX Inlet | | 7.2 | 229 | 293 | 11.9 | 300 | 18 | 383 | 15.6 | | | | | |
| Pre Baseline RX Outlet | | 8.7 | 225 | 291 | 11.7 | 331 | 23 | 428 | 17.2 | | | | | |
| Test 4 | 150 | 8.7 | 273 | 60 | 9.5 | 398 | 27 | 88 | 13.9 | 18.3 | 283 | 76 | 0.58 | 24.0 |
| Post Baseline RX Outlet | | 9.6 | 207 | 291 | 12.3 | 327 | 32 | 460 | 19.4 | | | | | |
| Post Baseline RX Inlet | | 8.1 | 207 | 289 | 12.1 | 290 | 31 | 405 | 16.7 | | | | | |

**Table 10. Detailed Results of the LoTOx™ Tests with Sub bituminous at High Temperature** **Test Date: 3.15.07**

| | Reactor Temp. °F | $O_2$ % | $SO_2$ ppm | NOx ppm | Hg (E) µg/m³ | $SO_2$ @3% $O_2$ ppm | CO @3% $O_2$ ppm | NOx @3% $O_2$ ppm | NOx Baseline ppm | Hg (E) @3% $O_2$ µg/m³ | Hg (E) Baseline µg/m³ | Ozone Flue Gas ppm | Excess Ozone ppm | Residence Time second | NOx % Red. | Hg (E) % Red. |
|---|---|---|---|---|---|---|---|---|---|---|---|---|---|---|---|---|
| Pre Baseline RX Inlet | | 5.7 | 298 | 207 | 10.8 | 350 | 17.5 | 244 | | 14.2 | | | | | | |
| Pre Baseline RX Outlet | | 7.3 | 298 | 204 | 11.2 | 390 | 19.7 | 268 | | 16.4 | | | | | | |
| Test 5 | 275 | 7.7 | 411 | 21 | 2.7 | 556 | 23.7 | 28 | 310 | 4.0 | 15.9 | 539 | 71 | 6.2 | 90.9 | 74.9 |
| Post Baseline RX Outlet | | 8.3 | 263 | 249 | 9.2 | 372 | 23.6 | 353 | | 15.5 | | | | | | |
| Post Baseline RX Inlet | | 6.0 | 287 | 222 | 9.6 | 344 | 23.6 | 267 | | 13.3 | | | | | | |
| Pre Baseline RX Outlet | | 8.0 | 280 | 209 | 10.5 | 386 | 28.2 | 289 | | 15.7 | | | | | | |
| Test 6 | 275 | 8.4 | 867 | 2 | 1.4 | 1236 | 32.7 | 3 | 285 | 2.3 | 15.8 | 721 | 264 | 5.73 | 98.9 | 85.7 |
| Post Baseline RX Outlet | | 8.0 | 284 | 203 | 10.3 | 393 | 27.4 | 281 | | 15.9 | | | | | | |
| Post Baseline RX inlet | | 6.6 | 279 | 206 | 11.1 | 350 | 22.1 | 258 | | 13.9 | | | | | | |
| Pre Baseline RX outlet | | 7.8 | 275 | 215 | 9.9 | 374 | 23.0 | 292 | | 15.8 | | | | | | |
| Test 7 | 275 | 7.9 | 346 | 101 | 5.9 | 475 | 24.1 | 139 | 303 | 9.1 | 16.2 | 275 | 67 | 0.45 | 54.2 | 43.6 |
| Post Baseline RX outlet | | 7.8 | 274 | 229 | 12.2 | 374 | 24.5 | 314 | | 16.7 | | | | | | |
| Post Baseline RX Inlet | | 6.3 | 282 | 228 | 11.0 | 344 | 20.7 | 278 | | 14.9 | | | | | | |
| Pre Baseline RX Outlet | | 8.4 | 265 | 221 | 10.9 | 377 | 24.8 | 315 | | 17.3 | | | | | | |
| Test 8 | 275 | 8.6 | 923 | 31 | 4.3 | 1342 | 28.5 | 46 | 341 | 6.9 | 17.2 | 515 | 294 | 0.47 | 86.6 | 59.5 |
| Post Baseline RX Outlet | | 8.7 | 257 | 251 | 10.3 | 376 | 23.9 | 367 | | 17.1 | | | | | | |

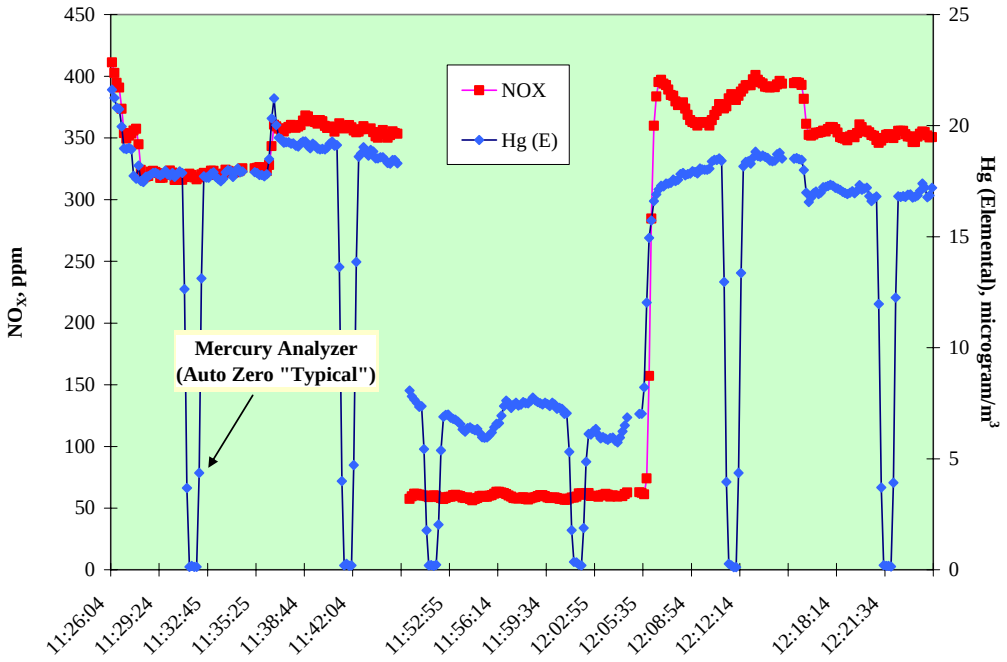


**Figure 10. Graphical Illustration of the Results of Test No. 1 with Bituminous Coal**

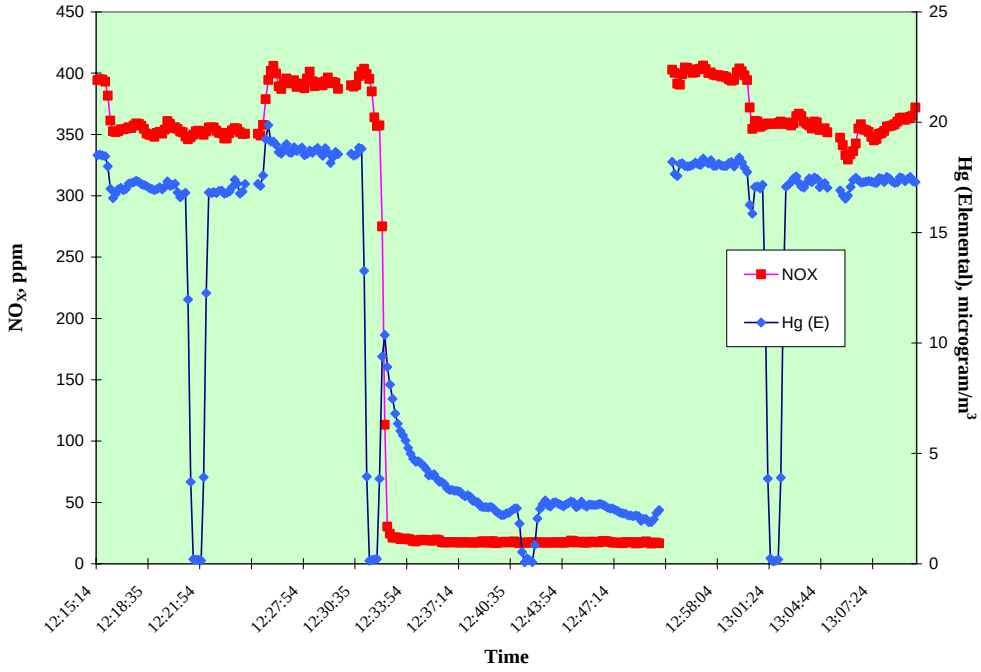


**Figure 11. Graphical Illustration of the Results of Test No. 2 with Bituminous Coal**

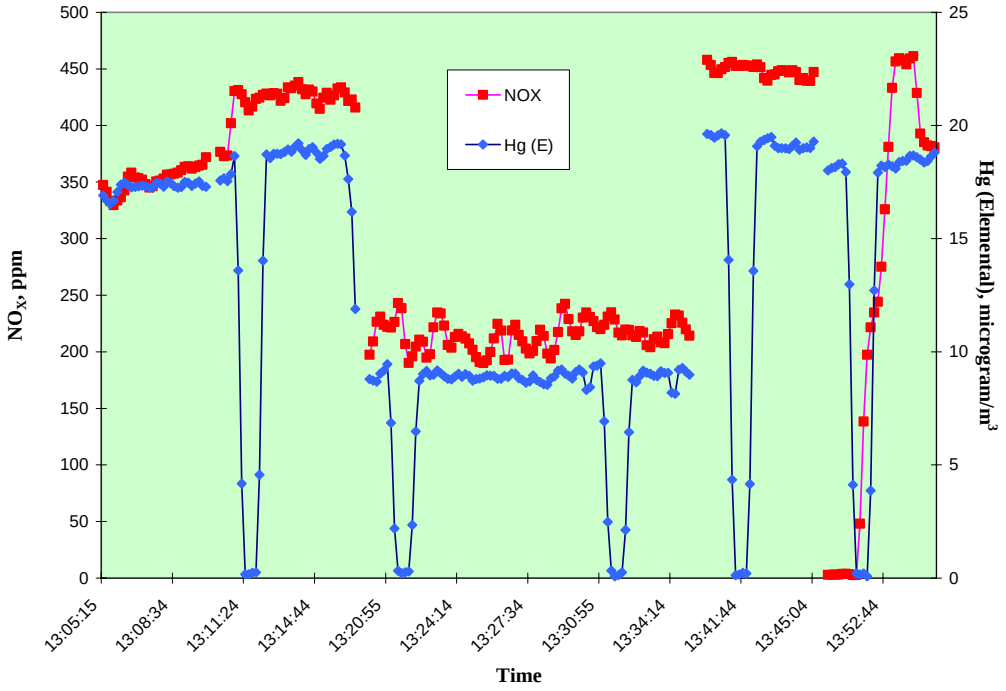


**Figure 12. Graphical Illustration of the Results of Test No. 3 with Bituminous Coal**

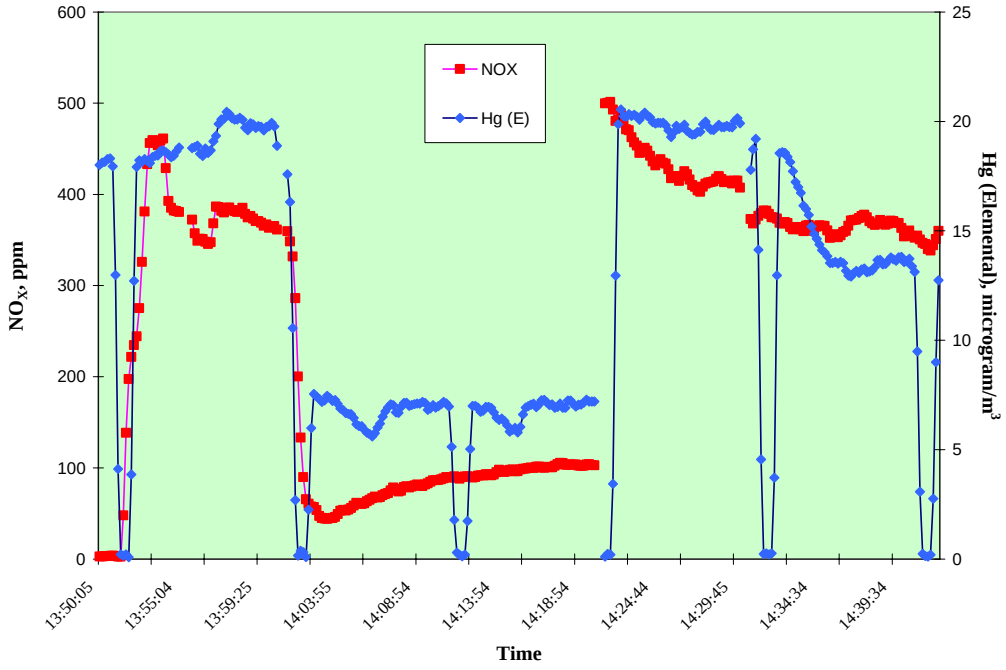


**Figure 13. Graphical Illustration of the Results of Test No. 4 with Bituminous Coal**

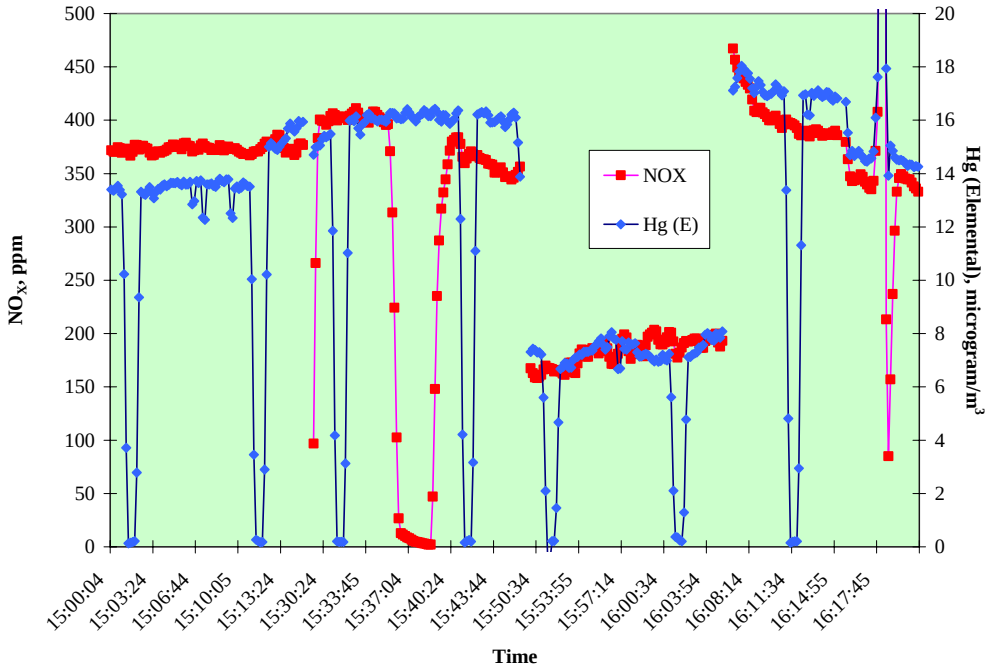


**Figure 14. Graphical Illustration of the Results of Test No. 5 with Bituminous Coal**

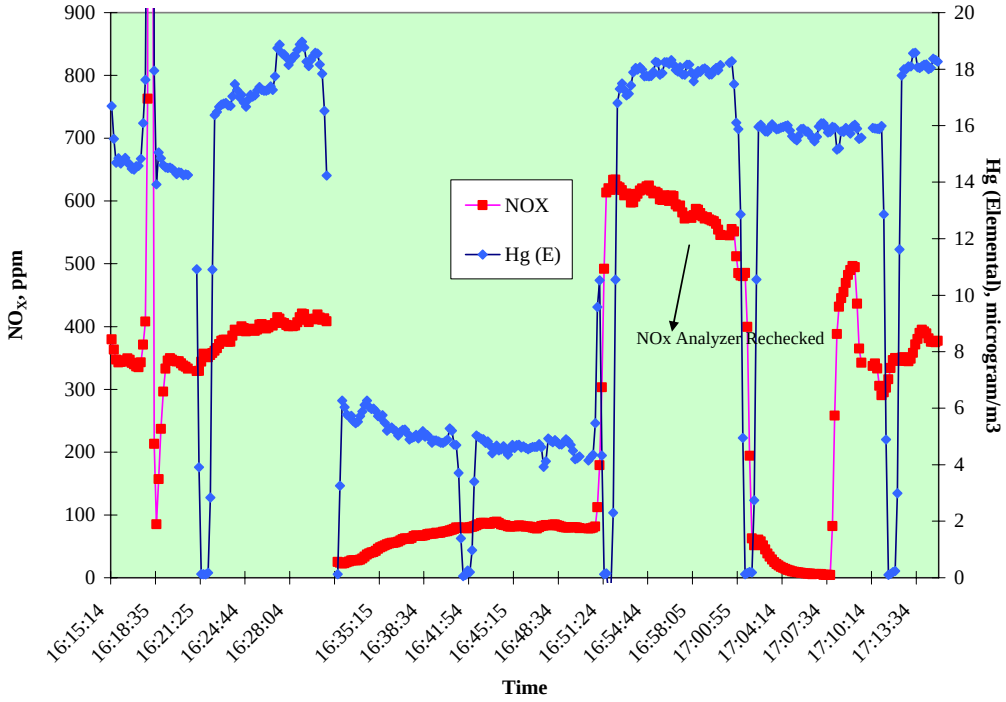


**Figure 15. Graphical Illustration of the Results of Test No. 6 with Bituminous Coal**

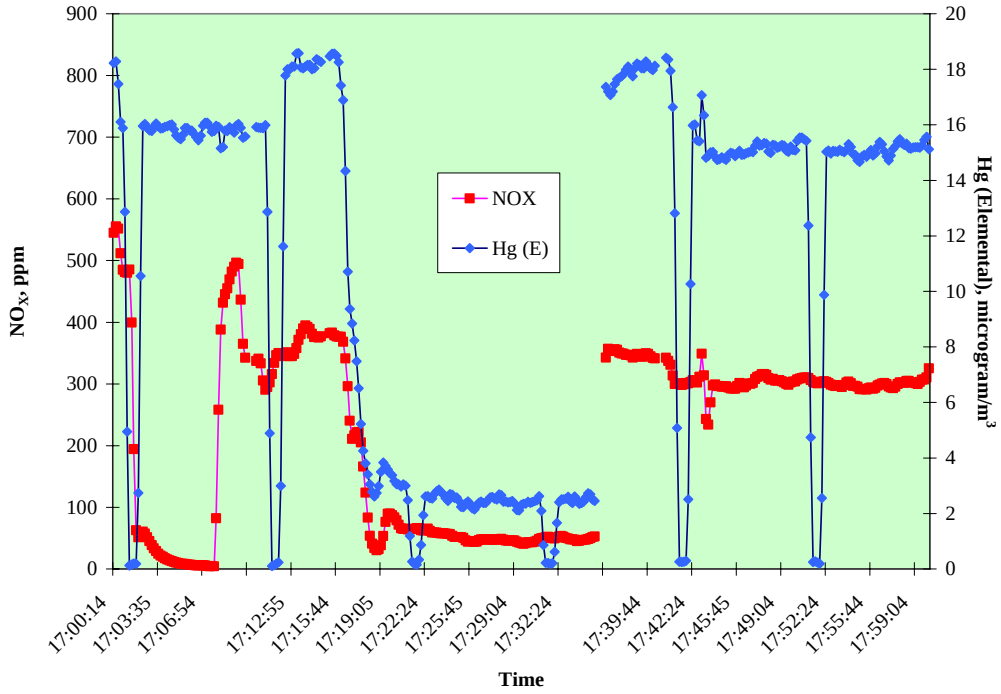


**Figure 16. Graphical Illustration of the Results of Test No. 7 with Bituminous Coal**

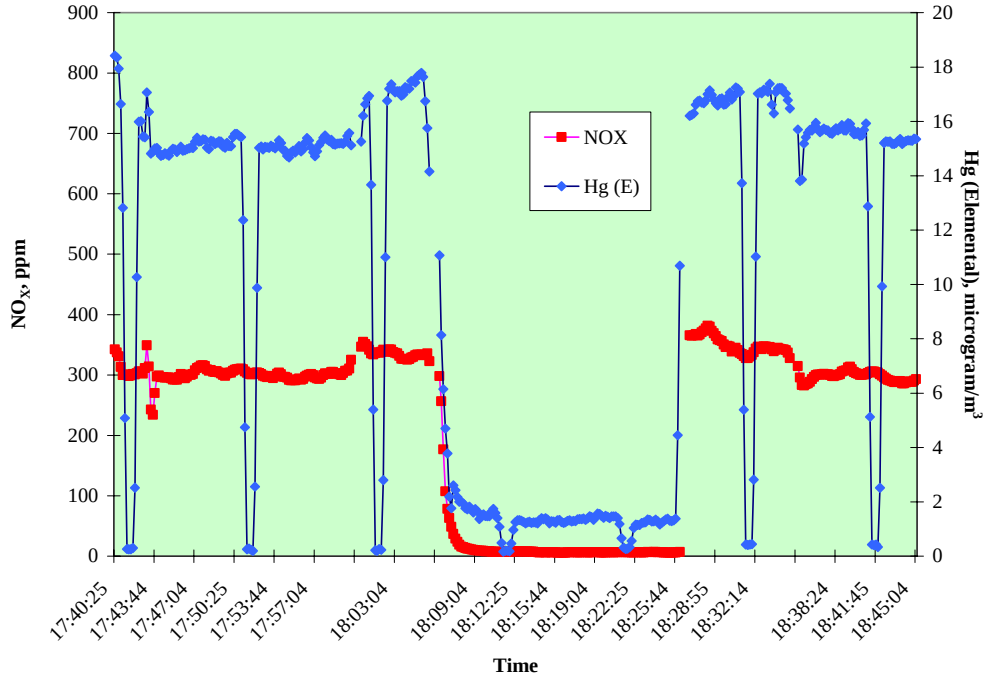


**Figure 17. Graphical Illustration of the Results of Test No. 8 with Bituminous Coal**

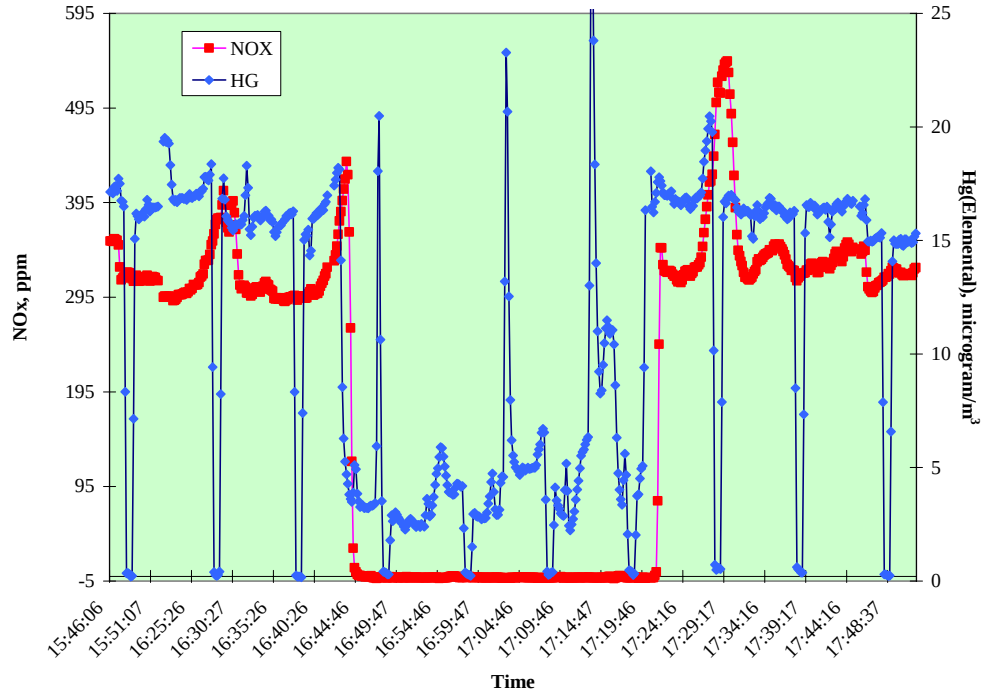


**Figure 18. Graphical Illustration of the Results of Test No. 1 with Subbituminous Coal**

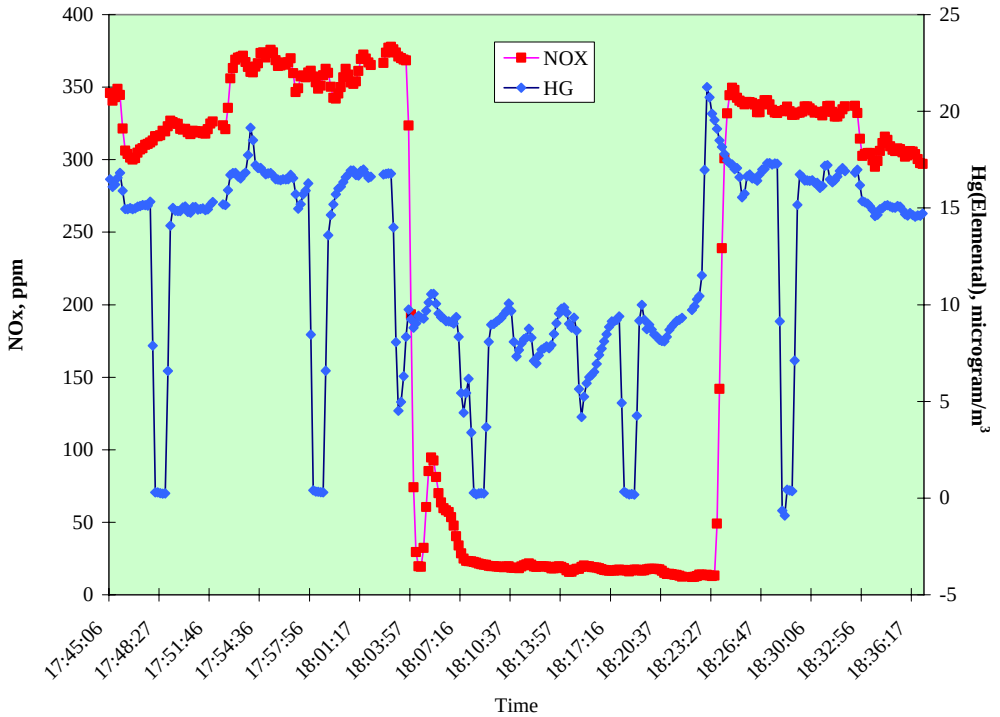


**Figure 19. Graphical Illustration of the Results of Test No. 2 with Subbituminous Coal**

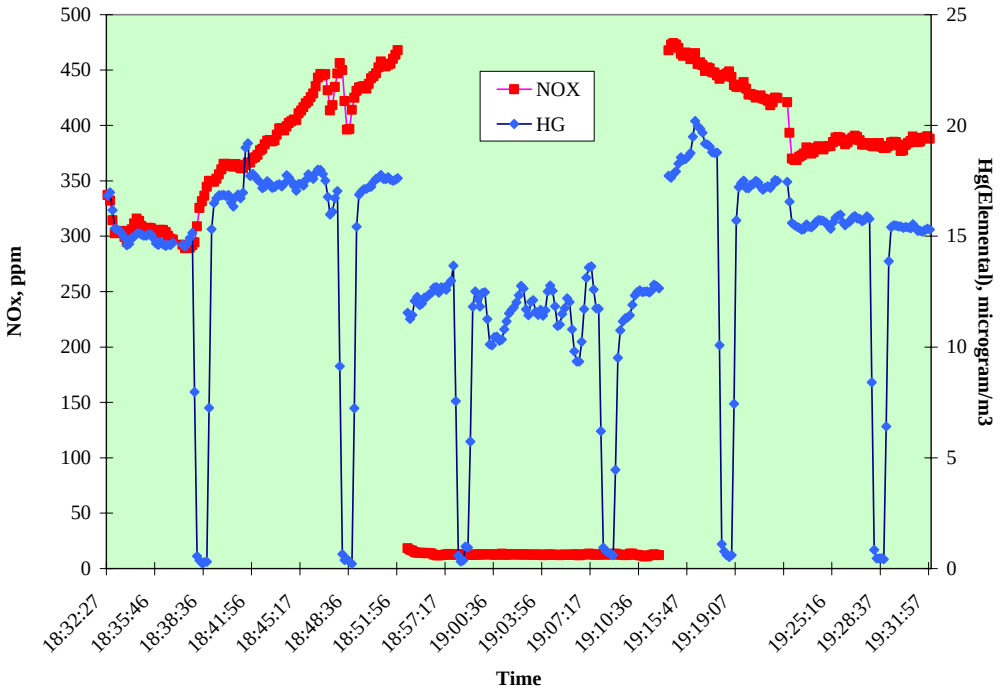


**Figure 20. Graphical Illustration of the Results of Test No. 3 with Subbituminous Coal**

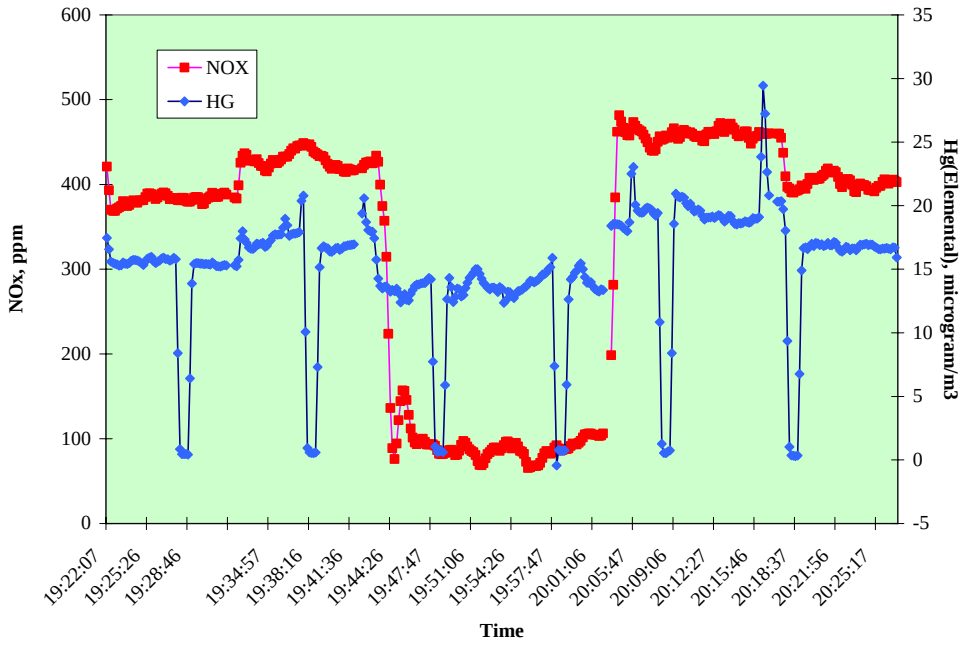


**Figure 21. Graphical Illustration of the Results of Test No. 4 with Subbituminous Coal**

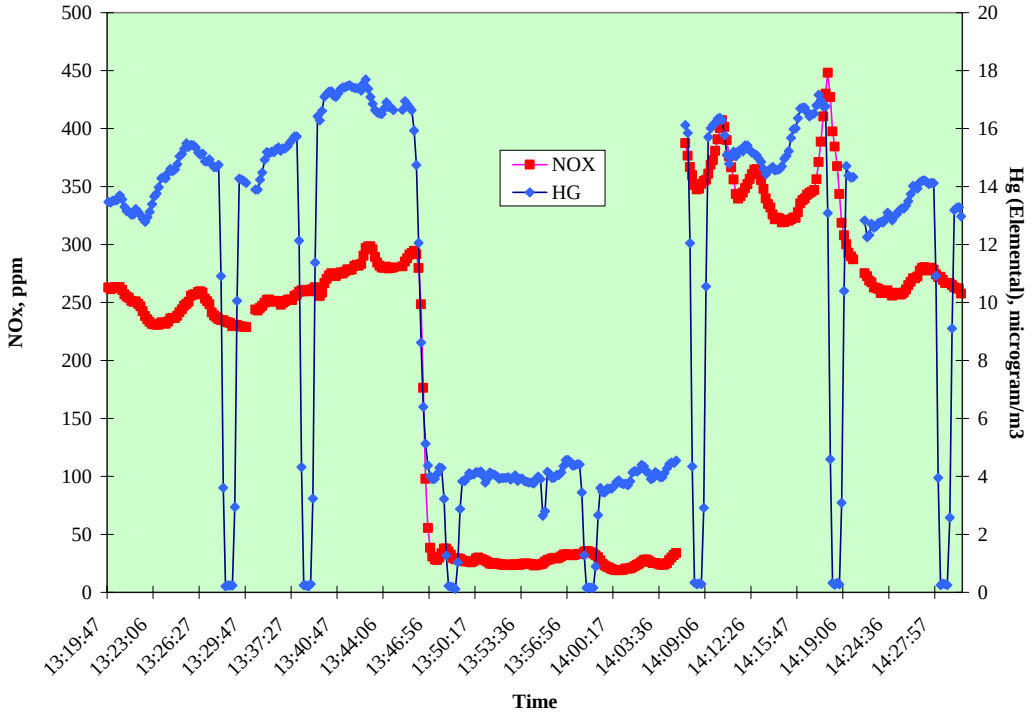


**Figure 22. Graphical Illustration of the Results of Test No. 5 with Subbituminous Coal**

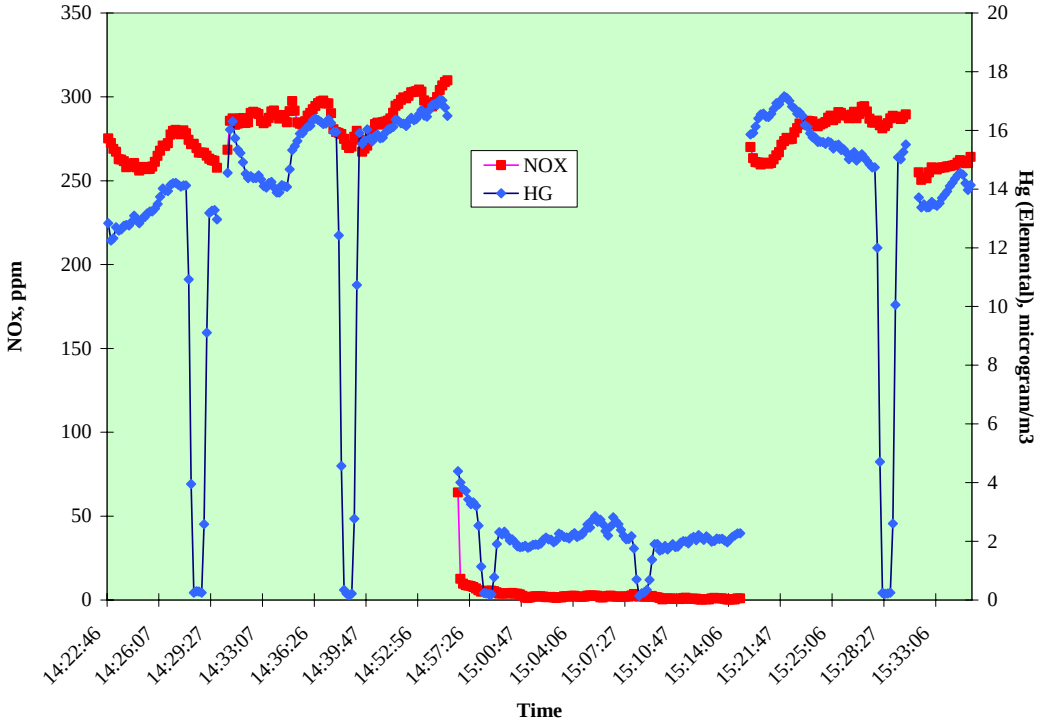


**Figure 23. Graphical Illustration of the Results of Test No. 6 with Subbituminous Coal**

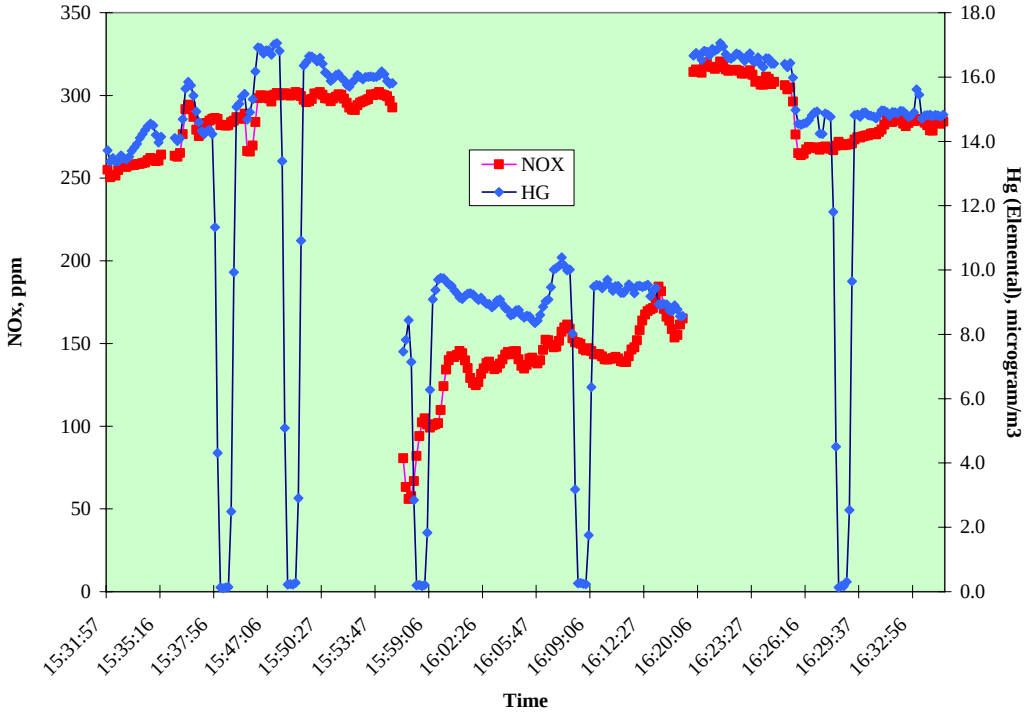


**Figure 24. Graphical Illustration of the Results of Test No. 7 with Subbituminous Coal**

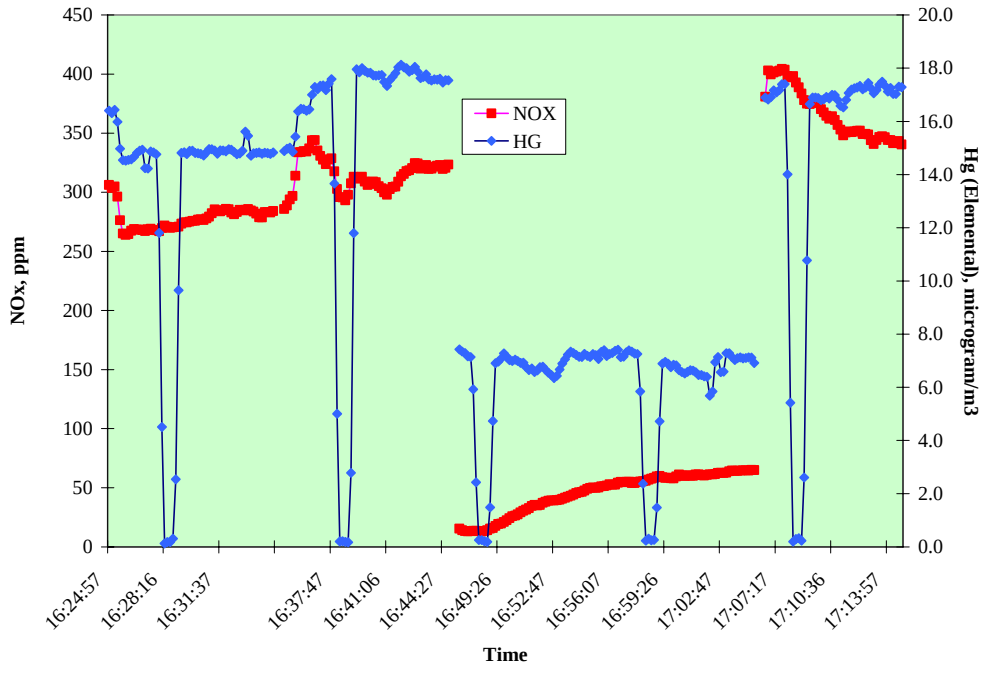


**Figure 25. Graphical Illustration of the Results of Test No. 8 with Subbituminous Coal**

# APPENDIX C

## Concentrations of Halogens and Halides in Flue Gas

## Method 26A
## Determination of Hydrogen Halide and Halogen Concentrations in the Flue Gas

This method is applicable for determining emissions of hydrogen halides (HCl, HBr, and HF) and halogens ($Cl_2$, $Br_2$, $F_2$) form stationary sources.

Method 26A is a proportional sampling procedure that uses large impingers to collect the sample. The concept of this method is based on extracting a sample from the source and passes it trough a pre purged heated probe and filter into diluted sulfuric acid and diluted sodium hydroxide solutions which collect the gaseous hydrogen halides and halogens, respectively. A schematic of the sampling train is presented in Figure 26. The hydrogen halides are solubilized in the acidic solution and form chloride ($Cl^-$), bromide ($Br^-$), and fluoride ($F^-$) ions. The halogens have a very low solubility in the acidic solution and passes through to the alkaline solution where they are hydrolyzed to form a proton ($H^+$) and halide ions, and the hypohalous acid (HClO or HBrO). Sodium thiosulfate is added in excess to the alkaline solution to assure reaction with the hypohalous acid to form a second halide ion such that two halides ions are formed for each molecule of halogen gas. The halide ions in the separated solutions are measured by ion chromatography.

The results of applying Method 26A for determining the concentration of halogens and halides present in the flue gas that is produced from the combustion of bituminous and subbituminous coal used in these test are presented in Table 11.

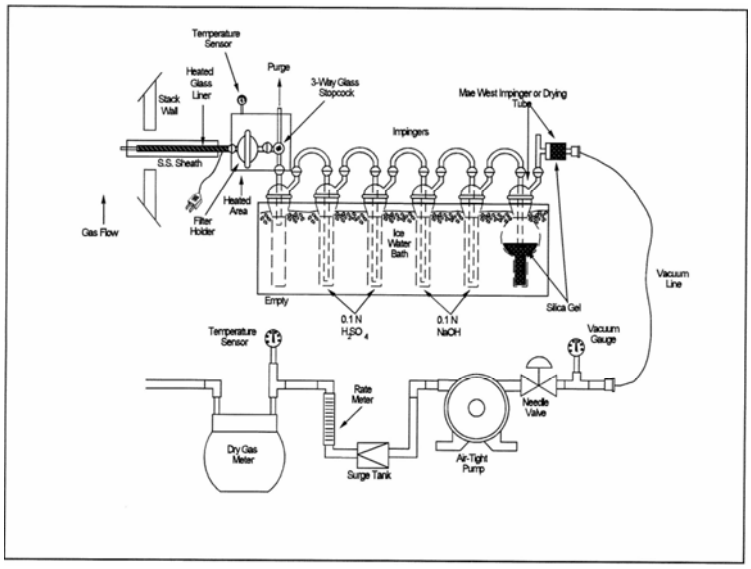


**Figure 26. Sampling Train for Method 26A**

**Table 11. Concentrations of Halides and Halogens in Flue Gas**
**Results of Method 26A (Halogens and Halides)**

| | Coal | Bituminous | Bituminous | Sub bituminous (Wyodak) | Sub bituminous (Wyodak) | Sub bituminous (Wyodak) |
|---|---|---|---|---|---|---|
| | Test Data | 3.7.08 | 3.7.08 | 3.14.07 | 3.15.07 | 3.15.09 |
| | Units | Run 1 | Run 2 | Run 1 | Run 2 | Run 3 |
| **HCl, HBr and HF Results** | | | | | | |
| HCl concentrations in gas - std. | $mg/m^3$ gas | 112.9 | 203.2 | 1.8 | 10.8 | 8.5 |
| HCl concentrations in gas | ppm | 76.7 | 138.0 | 1.2 | 7.3 | 5.7 |
| HBr concentrations in gas - std. Units | $mg/m^3$ gas | 0.6 | 0.8 | 0.0 | 0.0 | 0.0 |
| HBr concentrations in gas | ppm | 0.2 | 0.2 | 0.0 | 0.0 | 0.0 |
| HF Concentrations in gas - std. | $mg/m^3$ gas | 1.5 | 2.2 | 0.0 | 0.0 | 0.0 |
| HF concentrations in gas | ppm | 1.8 | 2.6 | 0.0 | 0.0 | 0.0 |
| **$Cl_2$ and $Br_2$ Results** | | | | | | |
| $Cl_2$ concentrations in gas - std. Units | $mg/m^3$ gas | 16.1 | 13.1 | 10.6 | 8.7 | 8.7 |
| $Cl_2$ concentrations in gas | ppm | 5.6 | 4.6 | 3.7 | 3.0 | 3.0 |
| $Br_2$ concentrations in gas - std. Units | $mg/m^3$ gas | 0.0 | 2.0 | 1.1 | 0.7 | 0.9 |
| $Br_2$ concentrations in gas | ppm | 0.0 | 0.3 | 0.2 | 0.1 | 0.1 |

Note: Run No. 2 with bituminous coal is unreliable due to backflow of impinger fluids

# APPENDIX D

## Evaluation of the Ozone Destruction Unit

Evaluation of the Ozone Destruction Unit

Due to the interference of the ozone with mercury measurements, a method was developed by Linde to destruct the ozone at high temperature (i.e., 550 $^{o}$F) before directing the sample to the mercury analyzer. This method was used in their evaluation of the LoTOx$^{TM}$ process using simulated flue gas. The same method and apparatus was utilized in the tests conducted at WRI using flue gas generated from coal combustion that was spiked with elemental mercury, however, evidence proved that additional mercury oxidation is taking place in part of the ozone destruction unit and therefore increased the uncertainty in residence time reported to some extent. The objectives are to determine the effect of the ozone destruction temperature in mercury measurements and the degree of uncertainty in the reported residence time.

Evaluation of the Effect of Ozone Destruction Temperature on Mercury Measurements

Several tests were conducted to evaluate the effect of ozone destruction temperature on mercury oxidation. To ensure a uniform temperature through the reactor and a minimum residence time, a new test apparatus for ozone destruction was utilized. A schematic of the apparatus used is shown in Figure 27. The Apparatus consists of two U-tubes made of 1/8" OD stainless tube that is heat traced and insulated with each section has its own temperature controller. The temperature was controlled after two-inch from the mixing location of the oxygen and the gas sample to ensure a uniform temperature throughout the reactor. The degree of oxidation of elemental mercury was measured as a function of ozone destruction temperature. A summary of the results are listed in Table 12.

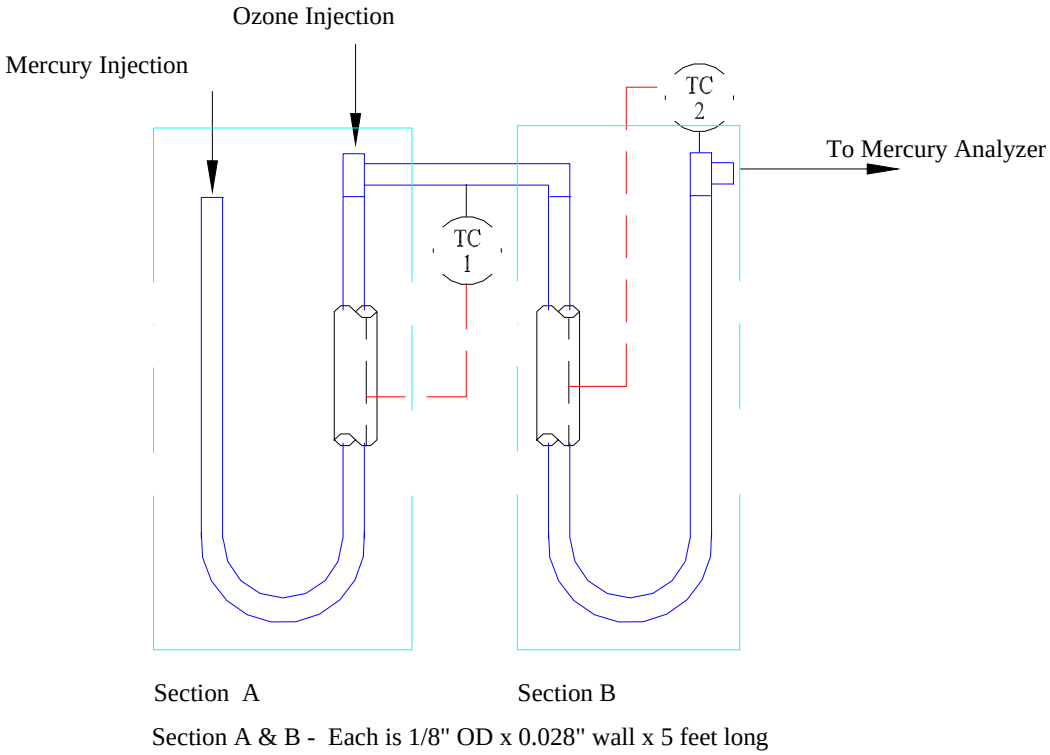


**Figure 27. Ozone Destruction Test Apparatus**

**Table 12. Evaluation of the Ozone Destruction Unit**

| Ozone | Hg(E) μg/m$^3$ | T $^o$F | Hg(E) % Reduction | Oxygen Flow Rate, slpm | % Weight Ozone in Oxygen | Sample Flow Rate, slpm | Flow Ratio $O_2$/Sample |
|---|---|---|---|---|---|---|---|
| OFF | 22.6 | 600 | | | | | |
| ON | 12.1 | 600 | 46.5 | 0.08 | 4.26 | 1.7 | 21 |
| OFF | 24.2 | 600 | | | | | |
| OFF | 28.9 | 658 | | | | | |
| ON | 21.4 | 653 | 26.0 | 0.08 | 4.26 | 1.6 | 19 |
| ON | 27.3 | 674 | | | | | |
| OFF | 31.2 | 675 | 12.5 | 0.08 | 4.26 | 1.6 | 19 |
| OFF | 31.4 | 700 | | | | | |
| ON | 26.3 | 700 | 16.2 | 0.08 | 4.26 | 1.5 | 19 |
| ON | 21.2 | 696 | | | | | |
| OFF | 23.2 | 696 | 8.8 | 0.02 | 4.65 | 1.4 | 71 |
| OFF | 24.0 | 591 | | | | | |
| ON | 21.7 | 594 | 20.7 | 0.02 | 4.61 | 1.4 | 71 |
| OFF | 23.6 | 700 | | | | | |
| ON | 20.5 | 700 | 13.1 | 0.02 | 4.87 | 1.4 | 71 |
| OFF | 25.2 | 750 | | | | | |
| ON | 25.2 | 750 | 0.2 | 0.02 | 4.76 | 1.4 | 71 |
| OFF | 25 | 750 | | | | | |

As indicated from the results, at 750 $^o$F gas temperature, a negligible oxidation of mercury was observed. Even though operating at 560 $^o$F was sufficient enough to destruct the ozone before it reaches to the mercury analyzer as was experienced in all the tests that were conducted with the quartz reactor, it was not sufficient enough to destruct the ozone instantaneously right after the mixing point. This behavior can be attributed to the wide difference in volume between the two ozone destruction units and according to the difference in residence time.

In order to determine the uncertainty in residence time, a new ozone destruction unit with a small internal volume (7 cm$^3$) was utilized for additional testing under similar conditions as the previous tests. The ozone destruction reactor was made from 1/8"OD x 0.028" wall x 6 feet long. The tube was heat traced to control the exist temperature of flue gas from the ozone destruction reactor at 750 $^o$F. The test conditions applied are based on utilizing a slip steam of flue gas generated from the combustion of subbituminous coal and operating the LoTOx$^{TM}$ unit at 150 $^o$F reactor temperature, high residence time, and an $O_3$/NOx stoichiometric ratio below 2.0. The results of these tests are presented in Table 13. Figure 28 shows all the results conducted with subbituminous coal utilizing the old quartz and the new stainless steel ozone destruction reactors. As indicated, the results from using both types of ozone destruction units are comparable in most of the cases (67%). The deviations observed with the remaining 33% of the results were attributed to the change in the baseline of mercury level when comparing its concentration before and after ozone injection. To better explain it, the calculation of the percentage reduction in elemental mercury is based on the following formulas

$$\mathrm{Hg(E)}_{\text{baseline}} = \frac{[\mathrm{Hg(E)}_{\text{outlet from the reactor before ozone injection}} - \mathrm{Hg(E)}_{\text{outlet from the reactor after ozone injection}}]}{2}$$

$$\%\ \mathrm{Hg(E)\,Reduction} = \frac{[\mathrm{Hg(E)}_{\text{baseline}} - \mathrm{Hg(E)}_{\text{with ozone injection}}]}{\mathrm{Hg(E)}_{\text{baseline}}} \text{ x } 100$$

The variation of the outlet concentration of baseline Hg (E) (with no ozone injection) from the ozone destruction reactor before and after ozone injection is dependent on the type of ozone destruction unit utilized. The quartz reactor shows a higher stability in comparison to the stainless steel even thought the stainless steel reactor was maintained at an exit temperature of flue gas sample of 750 $^{o}$F compare to 550 $^{o}$F for the quartz reactor. After certain period of time (i.e., two hours of testing) from passing the mercury across the stainless steel reactor, a noticeable decline in Hg (E) level in the exit stream from the ozone destruction unit during baseline in comparison to the baseline inlet mercury concentration to the main reactor. For that reason, data point where there is a wide variation in the baseline of mercury before and after ozone injection is not considered reliable. These data are marked with red arrows in Figure 29. The conclusion from this experiment is that the results from the ozone destruction units' tests utilizing the large volume quartz units and the small volume stainless steel are comparable. Based on the internal volumes of both the quartz reactor (i.e., 47 $cm^3$) and stainless steel reactor (i.e., 7 $cm^3$) and the flow rate of flue gas through the mercury sampling line (i.e., 1.5 slpm), the estimated residence time in the ozone destruction units are 1.1 seconds, and 0.18 seconds respectively. However, since comparable results were achieved with both units, the estimated residence time is about 0.18 in the quartz ozone destruction unit.

## Table 13. Results of the Tests Conducted with the New Ozone Destruction Unit

**Subbituminous Coal** — **Test Date: 9.27.07**

| | Reactor Temp. °F | $O_3$/NOx | $O_2$ % | $SO_2$ ppm | NOx ppm | CO ppm | Hg µg/m³ | $SO_2$ @3%$O_2$ ppm | CO @3%$O_2$ ppm | NOx @3%$O_2$ ppm | NOx Avg. ppm | Hg (E) @3%$O_2$ µg/Nm³ | Hg (E) Avg. µg/m³ | Ozone Flue Gas ppm | Excess Ozone ppm | Residence Time seconds | NOx % Red. | Hg(E) % Red. |
|---|---|---|---|---|---|---|---|---|---|---|---|---|---|---|---|---|---|---|
| Baseline [ RX Inlet] | | | 10.8 | 190 | 212 | 41 | 11.2 | 334 | 72 | 374 | | 19.7 | | | | | | |
| Baseline [ RX Outlet] | | | 11.9 | 185 | 201 | 41 | 10.3 | 380 | 84 | 413 | | 21.1 | | | | | | |
| **Test 1** | 150 | 1.20 | 11.7 | 152 | 26 | 40 | 5.4 | 308 | 81 | 53 | 395 | 10.9 | 19.8 | 229 | 27 | 5.07 | 86.7 | 45.2 |
| Baseline [ RX Outlet] | | | 11.7 | 175 | 187 | 41 | 9.2 | 353 | 82 | 376 | | 18.5 | | | | | | |
| Baseline [ RX Inlet] | | | 10.4 | 186 | 195 | 41 | 11.9 | 314 | 70 | 332 | | 20.4 | | | | | | |
| Baseline [ RX Outlet] | | | 11.7 | 179 | 194 | 40 | 10.7 | 362 | 84 | 393 | | 20.6 | | | | | | |
| **Test 2** | 150 | 1.66 | 11.7 | 189 | 6 | 40 | 4.3 | 383 | 81 | 13 | 387 | 8.7 | 18.7 | 311 | 78 | 5.5 | 96.8 | 53.2 |
| Baseline [ RX Outlet] | | | 11.8 | 186 | 187 | 40 | 8.3 | 377 | 82 | 381 | | 16.8 | | | | | | |
| Baseline [ RX Inlet] | | | 10.4 | 205 | 189 | 41 | 11.4 | 347 | 69 | 320 | | 19.4 | | | | | | |

**Subbituminous Coal** — **Test Date: 10.3.07**

| | Reactor Temp. °F | O3/NOx | $O_2$ % | $SO_2$ ppm | NOx ppm | CO ppm | Hg µg/m³ | $SO_2$ @3%$O_2$ ppm | CO @3%$O_2$ ppm | NOx @3%$O_2$ ppm | NOx Baseline ppm | Hg (E) @3%$O_2$ µg/m³ | Hg (E) Baseline µg/m³ | Ozone Flue Gas ppm | Excess Ozone ppm | Residence Time seconds | NOx % Red. | Hg(E) % Red. |
|---|---|---|---|---|---|---|---|---|---|---|---|---|---|---|---|---|---|---|
| Baseline [RX Inlet] | | | 6.4 | 248 | 269 | 41 | 12.7 | 305 | 51 | 331 | | 15.7 | | | | | | |
| Baseline [RX Outlet] | | | 7.9 | 244 | 263 | 42 | 13.0 | 333 | 58 | 359 | | 17.7 | | | | | | |
| **Test 1** | 150 | 1.48 | 7.6 | 287 | 4 | 41 | 4.4 | 383 | 54 | 5.0 | 367 | 5.8 | 18.3 | 382 | 87 | 5.8 | 98.6 | 68.1 |
| Baseline [RX Outlet] | | | 8.4 | 229 | 261 | 42 | 13.3 | 328 | 60 | 374 | | 19.0 | | | | | | |
| Baseline [RX Inlet] | | | 7.3 | 234 | 268 | 42 | 14.7 | 309 | 56 | 353 | | 19.3 | | | | | | |
| Baseline [RX Outlet] | | | 7.9 | 237 | 261 | 43 | 13.2 | 326 | 59 | 360 | | 18.2 | | | | | | |
| **Test 2** | 150 | 1.28 | 9.1 | 239 | 5 | 41 | 4.9 | 364 | 62 | 7.5 | 373 | 7.5 | 19.3 | 437 | 39 | 7.4 | 98.0 | 61.3 |
| Baseline [RX Outlet] | | | 8.8 | 204 | 259 | 42 | 13.7 | 304 | 62 | 385 | | 20.4 | | | | | | |
| Baseline [RX Inlet] | | | 7.0 | 233 | 270 | 42 | 13.5 | 300 | 54 | 348 | | 17.4 | | | | | | |
| Baseline [RX Outlet] | | | 8.9 | 208 | 270 | 42 | 13.1 | 312 | 64 | 406 | | 19.7 | | | | | | |
| **Test 3** | 150 | 1.97 | 9.5 | 390 | 2 | 41 | 4.1 | 622 | 66 | 3.6 | 374 | 6.5 | 18.1 | 514 | 138 | 6.5 | 99.0 | 64.2 |
| Baseline [RX Outlet] | | | 9.1 | 199 | 260 | 41 | 10.8 | 306 | 64 | 341 | | 16.6 | | | | | | |
| Baseline [RX Inlet] | | | 7.6 | 207 | 267 | 42 | 13.6 | 279 | 56 | 359 | | 18.3 | | | | | | |
| | | | 8.1 | 172 | 213 | 42 | 11.8 | 245 | 59 | 303 | | 16.7 | | | | | | |

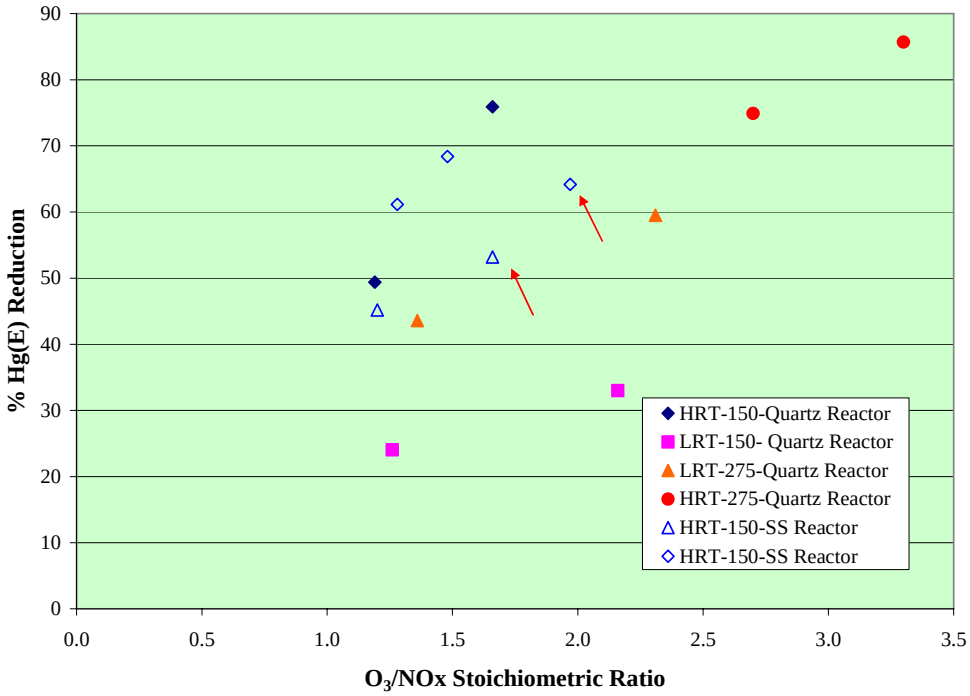


**Figure 28. Comparison of Hg(E) Reduction using Two Types of Ozone Destruction Units**

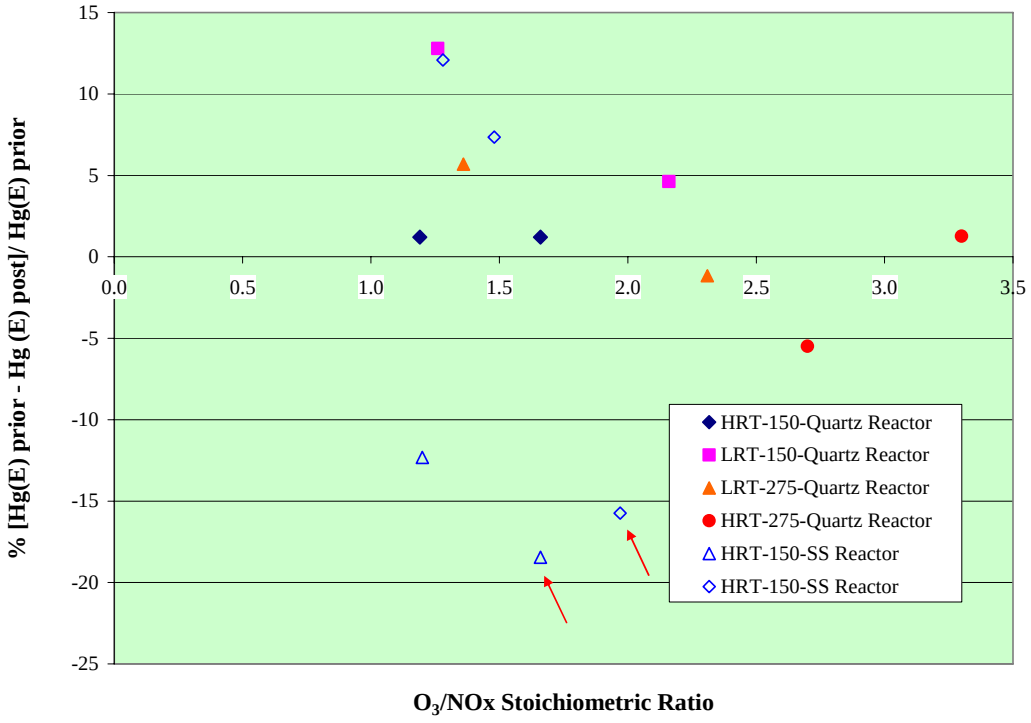


**Figure 29. Variation in Baseline of Hg(E) at the Exit Point from the Reactor with Two Types of Ozone Destruction Units**